Twinned *versus* Linked Organometallics - Bimetallic "Half-Baguette" Pentalenide Complexes of Rh(I)

Hugh J. Sanderson,[a] Gabriele Kociok-Köhn,[b] Claire L. McMullin,[a] Ulrich Hintermair*[a,c]

a) *Department of Chemistry, University of Bath, Claverton Down, Bath BA2 7AY, UK.*
b) *Material and Chemical Characterisation Facility, University of Bath, Claverton Down, Bath BA2 7AY, UK.*
c) *Institute for Sustainability, University of Bath, Claverton Down, Bath, BA2 7AY, UK.*

u.hintermair@bath.ac.uk

Supporting Information

Contents

Spectroscopic Data

Anti-[Rh^{I}(COD)]$_2$[μ:η^5:η^5Ph$_4$Pn] (**1**)

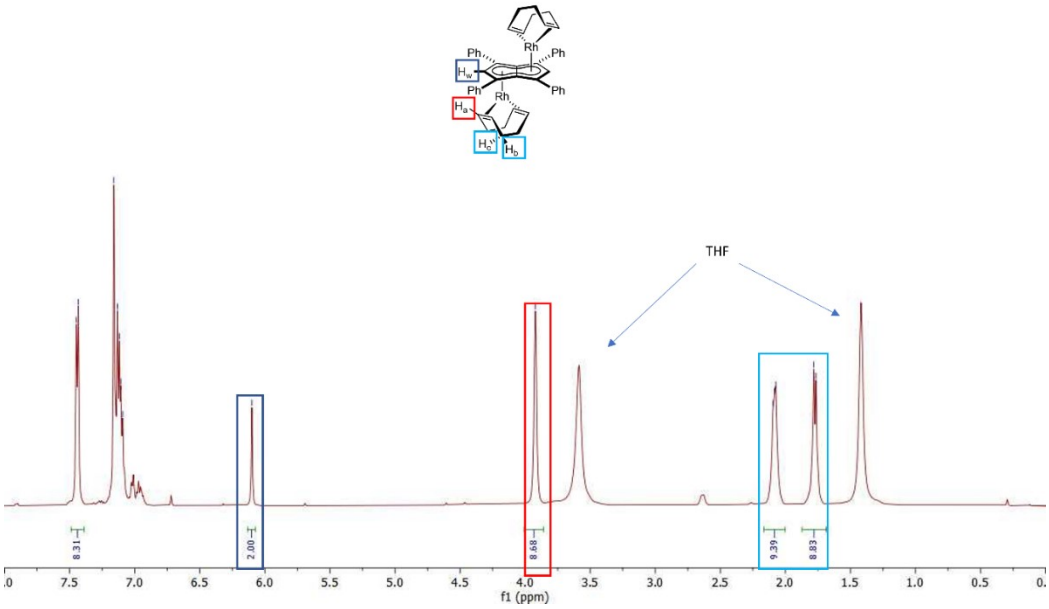

Figure S1: 500 MHz ^{1}H NMR spectrum of [Rh^{I}(COD)]$_2$[μ:η^5:η^5Ph$_4$Pn] in C_6D_6

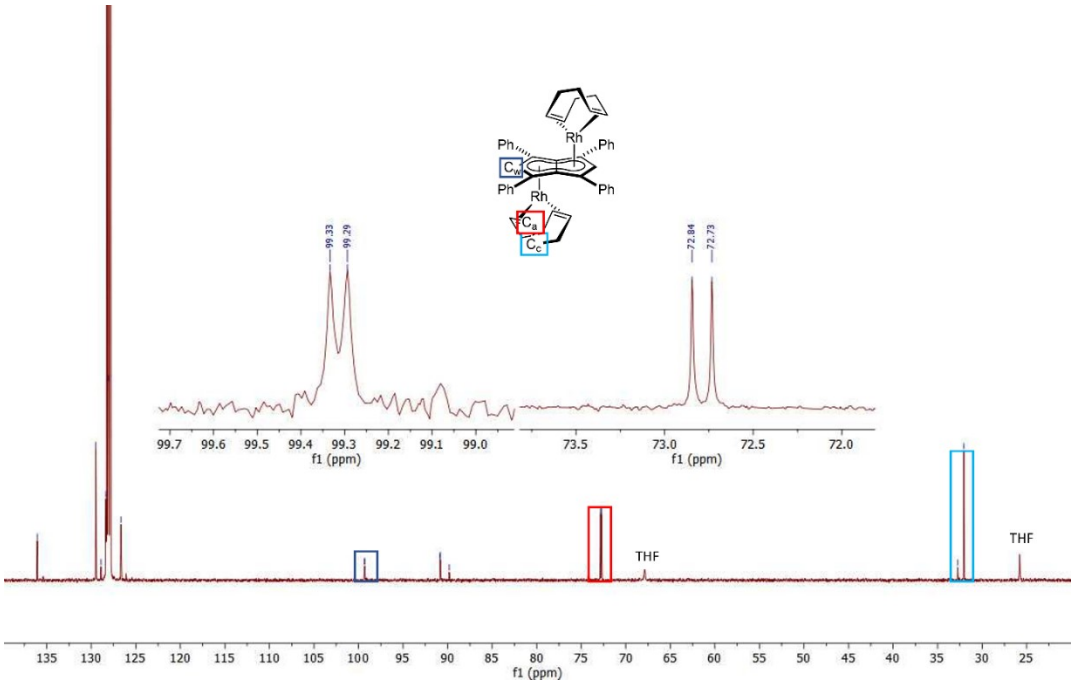

Figure S2: 126 MHz ^{13}C{^{1}H} NMR spectrum of [Rh^{I}(COD)]$_2$[μ:η^5:η^5Ph$_4$Pn] in C_6D_6

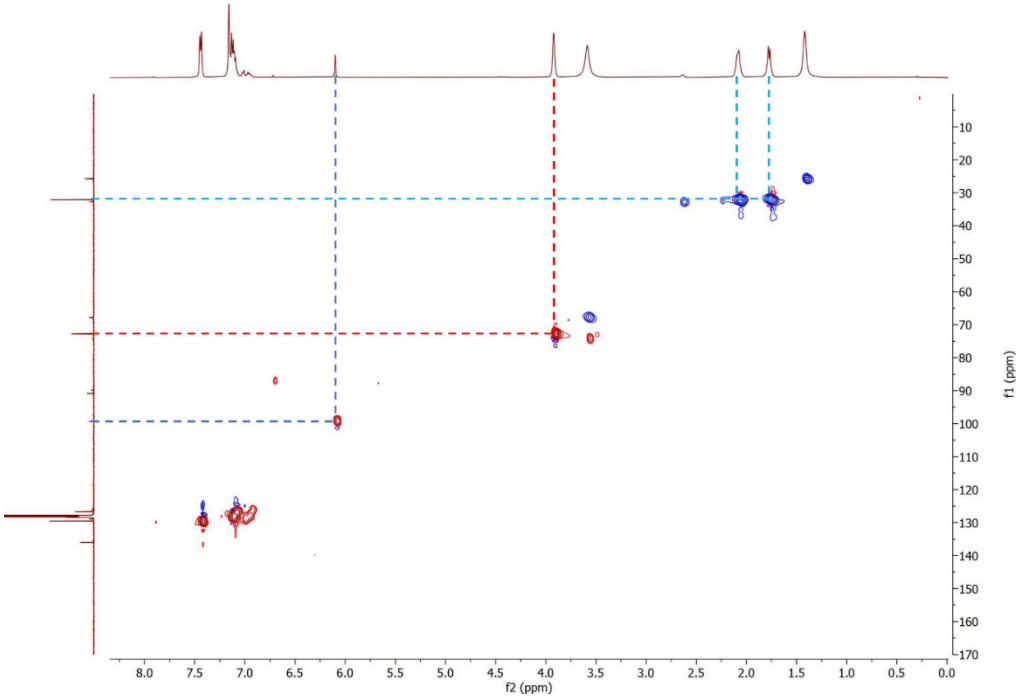

Figure S3: 500 MHz ^{1}H-^{1}H HSQC spectrum of $[Rh^{I}(COD)]_2[\mu:\eta^5:\eta^5Ph_4Pn]$ in C_6D_6 (Blue = H_w, Red = H_a, Light blue = H_b and H_c)

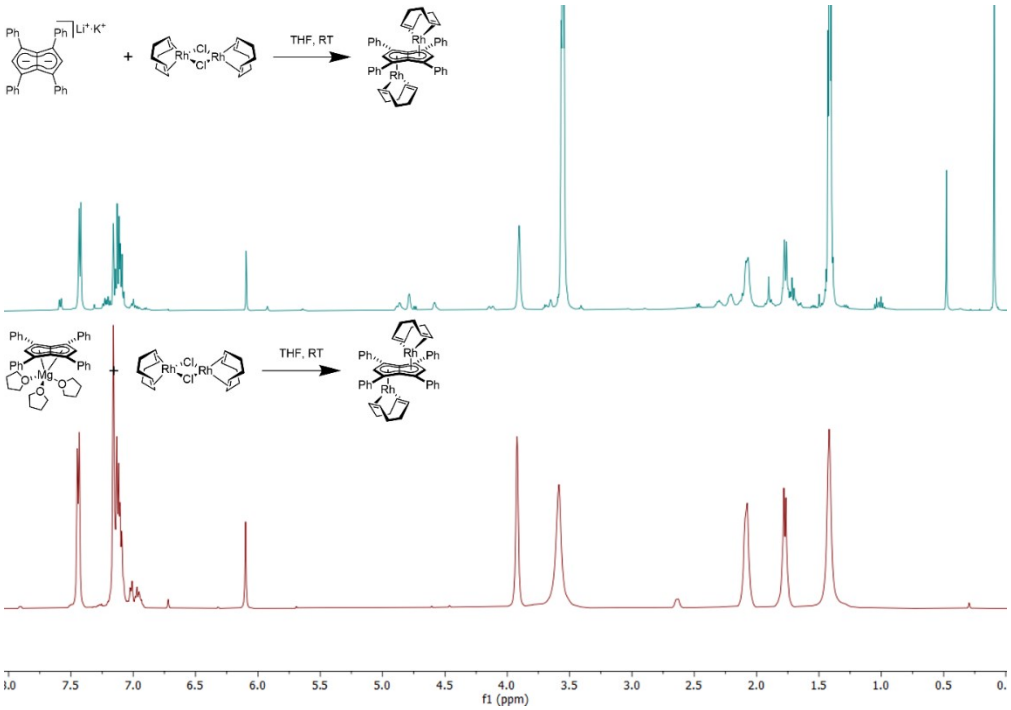

Figure S4: 500 MHz stacked ^{1}H NMR spectra of $[Rh^{I}(COD)]_2[\mu:\eta^5:\eta^5Ph_4Pn]$ in C_6D_6

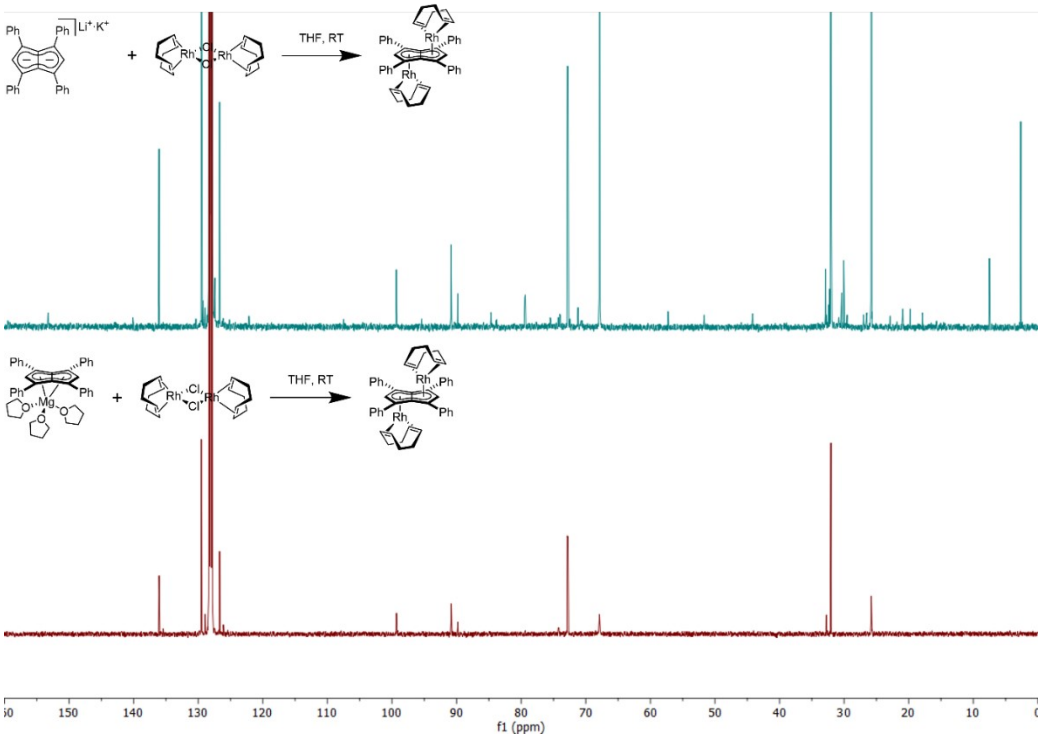

Figure S5: 126 MHz stacked $^{13}C\{^{1}H\}$ NMR spectra of $[Rh^{I}(COD)]_2[\mu:\eta^5:\eta^5Ph_4Pn]$ in C_6D_6

Anti-$[Ir^{I}(COD)]_2[\mu:\eta^5:\eta^5Ph_4Pn]$ (**2**)

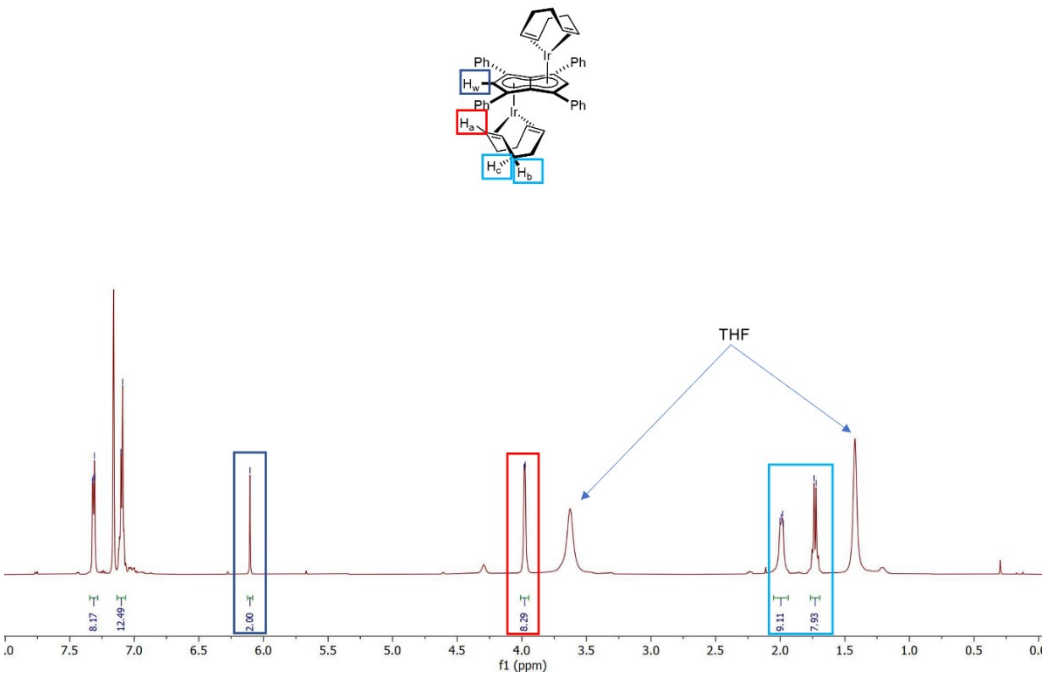

Figure S6: 500 MHz ^{1}H NMR spectrum of $[Ir^{I}(COD)]_2[\mu:\eta^5:\eta^5Ph_4Pn]$ in C_6D_6

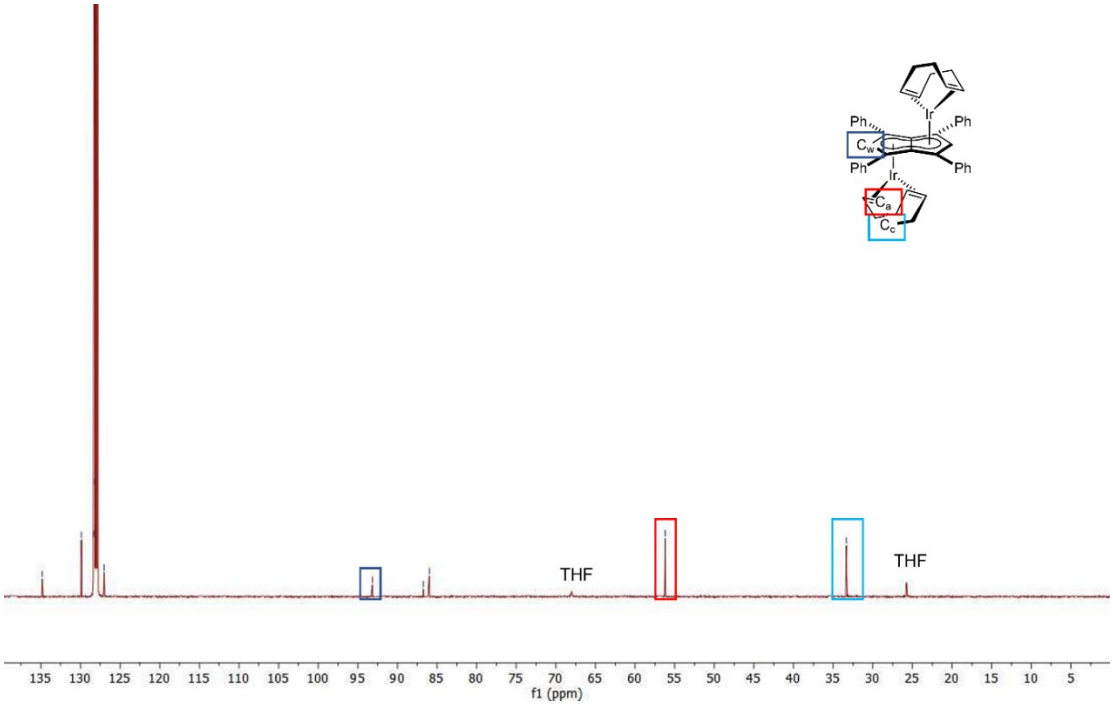

Figure S7: 126 MHz $^{13}C\{^{1}H\}$ NMR spectrum of $[Ir^{I}(COD)]_2[\mu:\eta^5:\eta^5Ph_4Pn]$ in C_6D_6

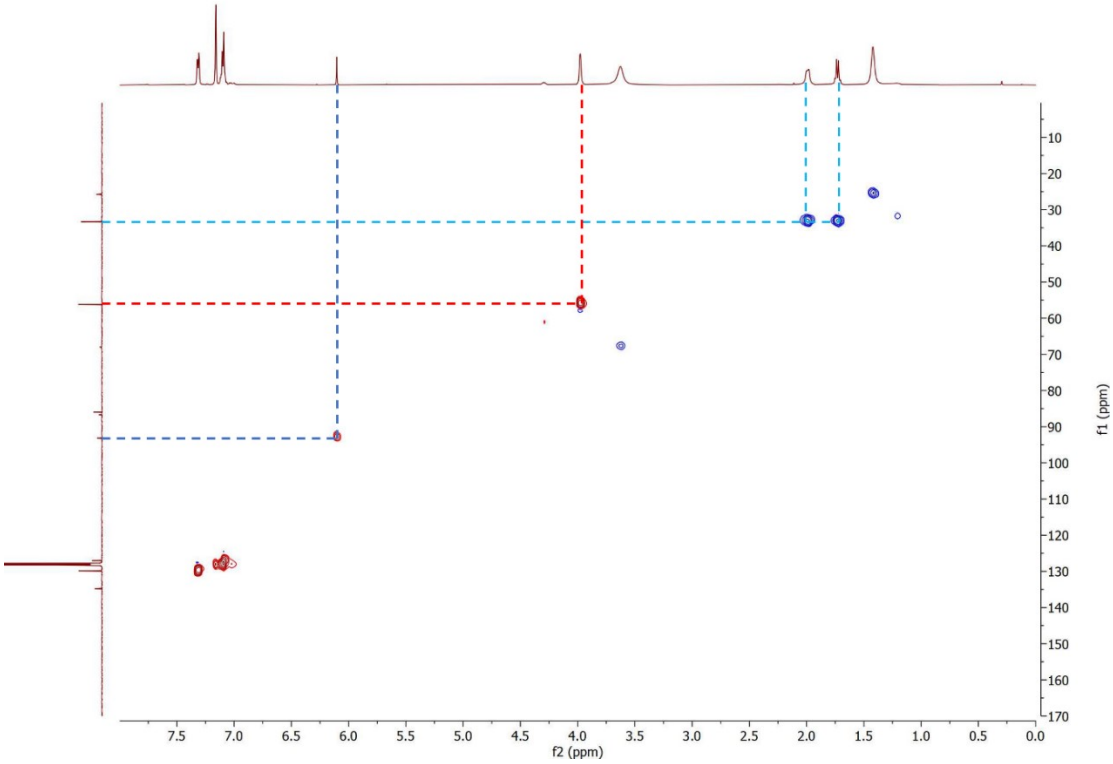

Figure S8: 500 MHz ^{1}H-^{13}C HSQC spectrum of $[Ir^{I}(COD)]_2[\mu:\eta^5:\eta^5Ph_4Pn]$ in C_6D_6 (Blue = H_w, Red = H_a, Light blue = H_b and H_c)

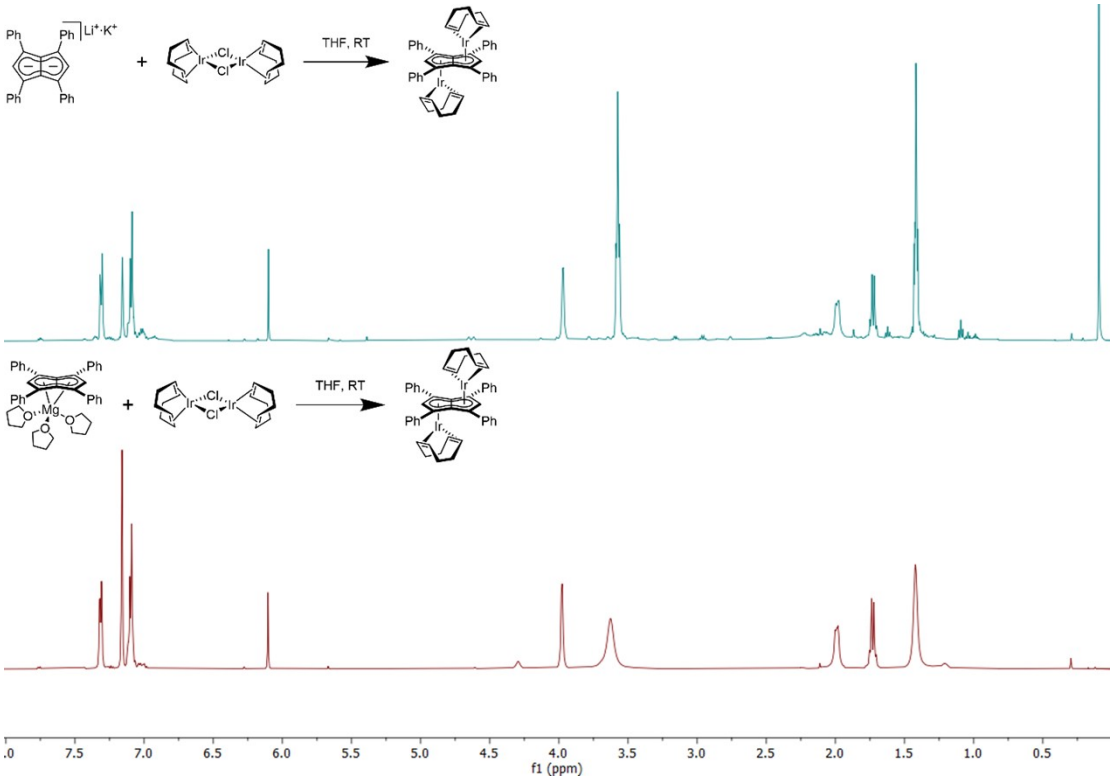

Figure S9: 500 MHz stacked ^{1}H NMR spectra of $[Ir^{I}(COD)]_2[\mu{:}\eta^5{:}\eta^5Ph_4Pn]$ in C_6D_6

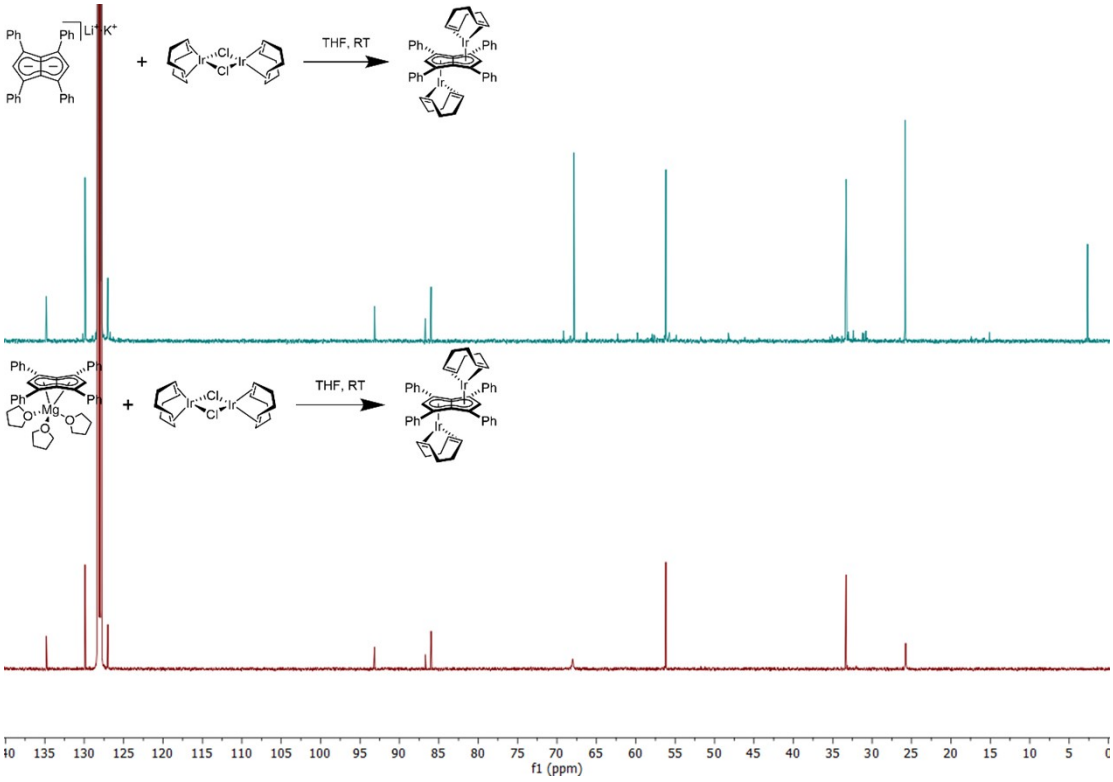

Figure S10: 500 MHz stacked ^{1}H NMR spectra of $[Ir^{I}(COD)]_2[\mu{:}\eta^5{:}\eta^5Ph_4Pn]$ in C_6D_6

Anti-[Rh^{I}(NBD)]$_2$[μ:η^5:η^5Ph$_4$Pn] (**3**)

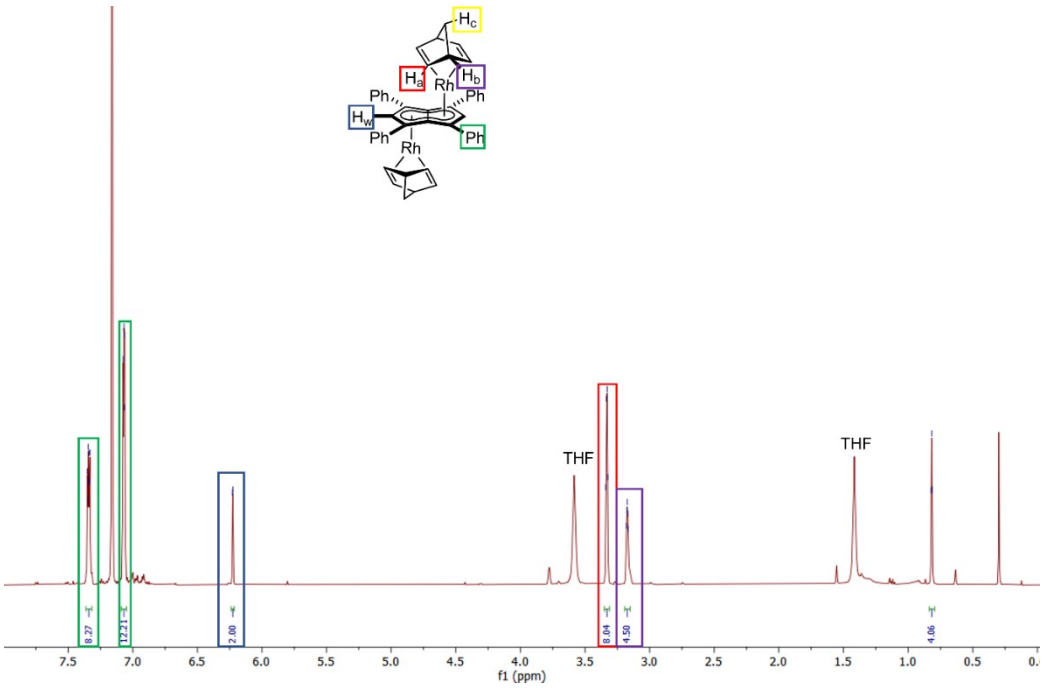

Figure S11: 500 MHz ^{1}H NMR spectrum of [Rh^{I}(NBD)]$_2$[μ:η^5:η^5Ph$_4$Pn] in C_6D_6

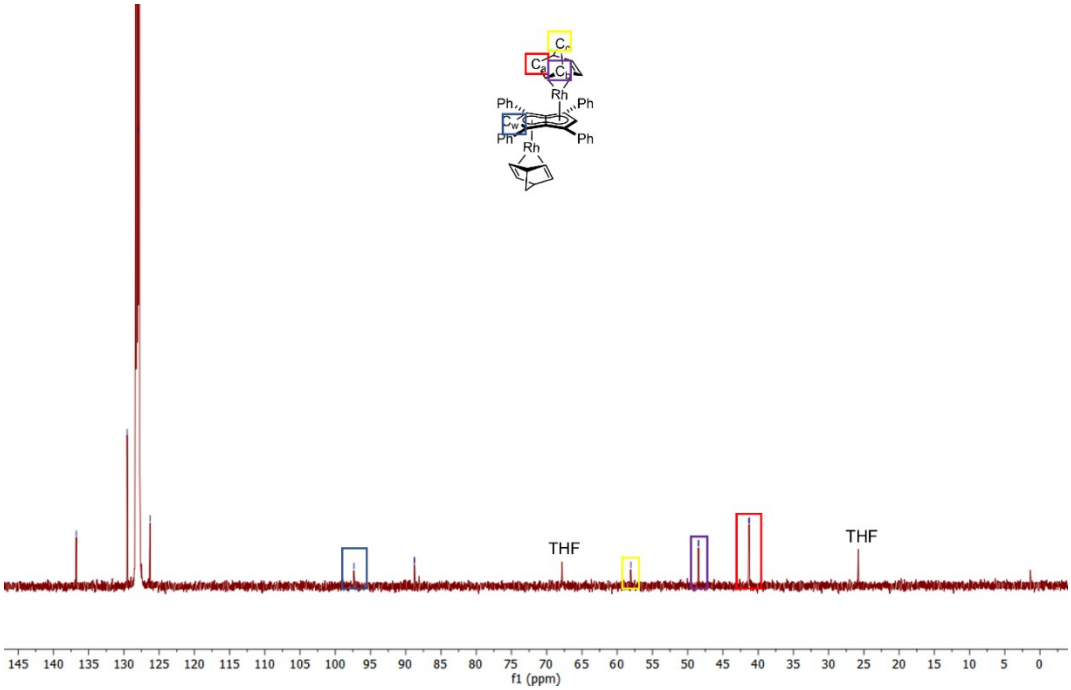

Figure S12: 126 MHz ^{13}C{^{1}H} NMR spectrum of [Rh^{I}(NBD)]$_2$[μ:η^5:η^5Ph$_4$Pn] in C_6D_6

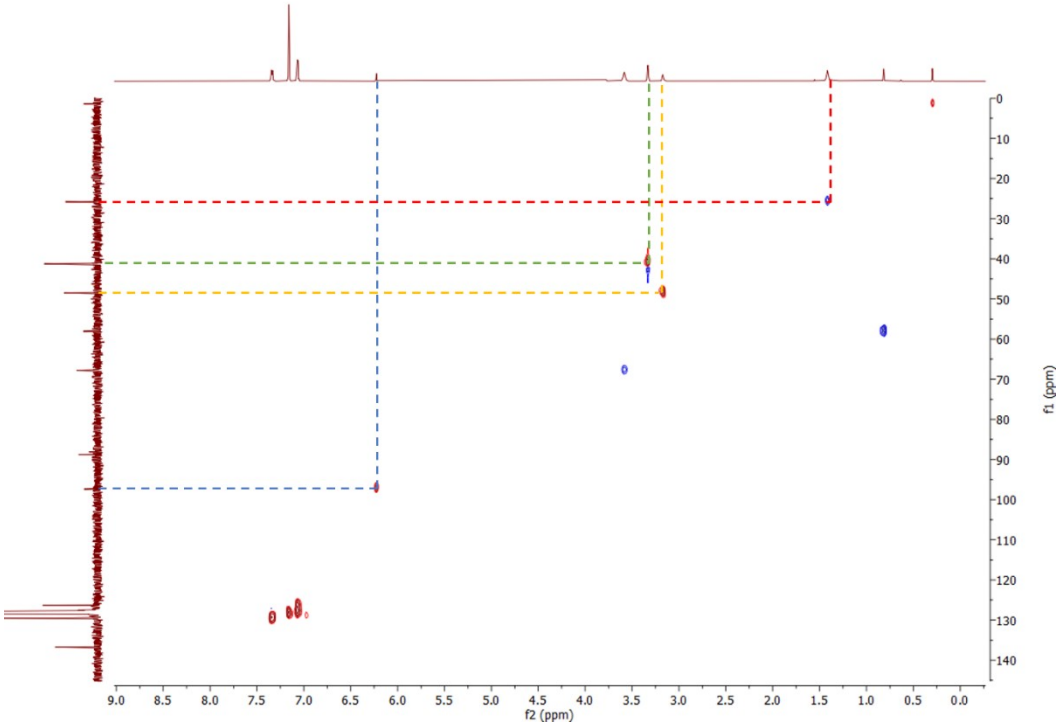

Figure S13: 500 MHz ^{1}H-^{13}C HSQC spectrum of $[Rh^{I}(NBD)]_2[\mu:\eta^5:\eta^5Ph_4Pn]$ in C_6D_6 (Blue = H_w, Yellow = H_b, Green = H_a, Red = H_c)

Anti-$[Rh^{I}(C_2H_4)_2]_2[\mu:\eta^5:\eta^5Ph_4Pn]$ (**4**)

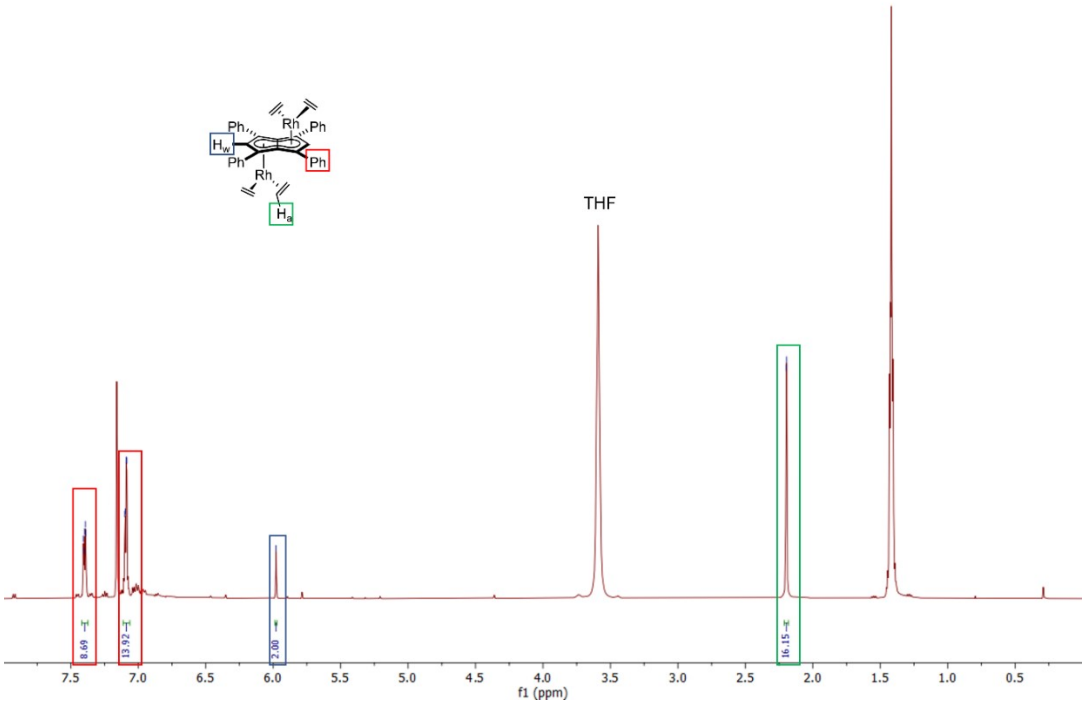

Figure S14: 500 MHz ^{1}H NMR spectrum of $[Rh^{I}(C_2H_4)_2]_2[\mu:\eta^5:\eta^5Ph_4Pn]$ in C_6D_6

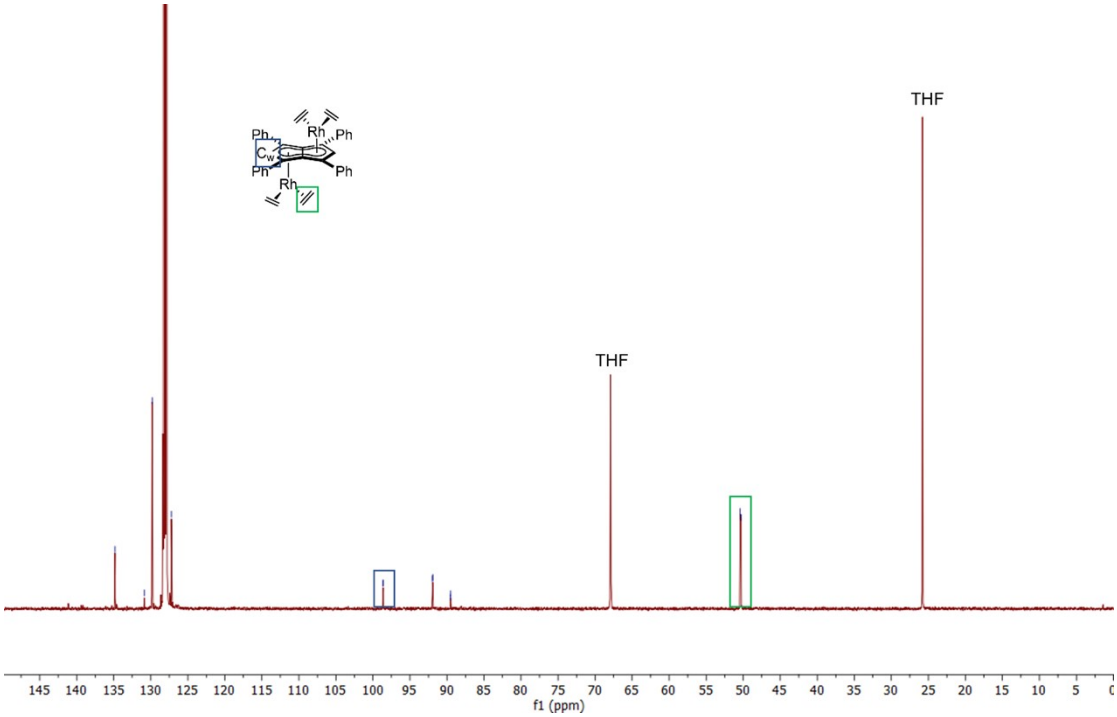

Figure S15 126 MHz $^{13}C\{^{1}H\}$ NMR spectrum of $[Rh^{I}(C_2H_4)_2]_2[\mu:\eta^5:\eta^5Ph_4Pn]$ in C_6D_6

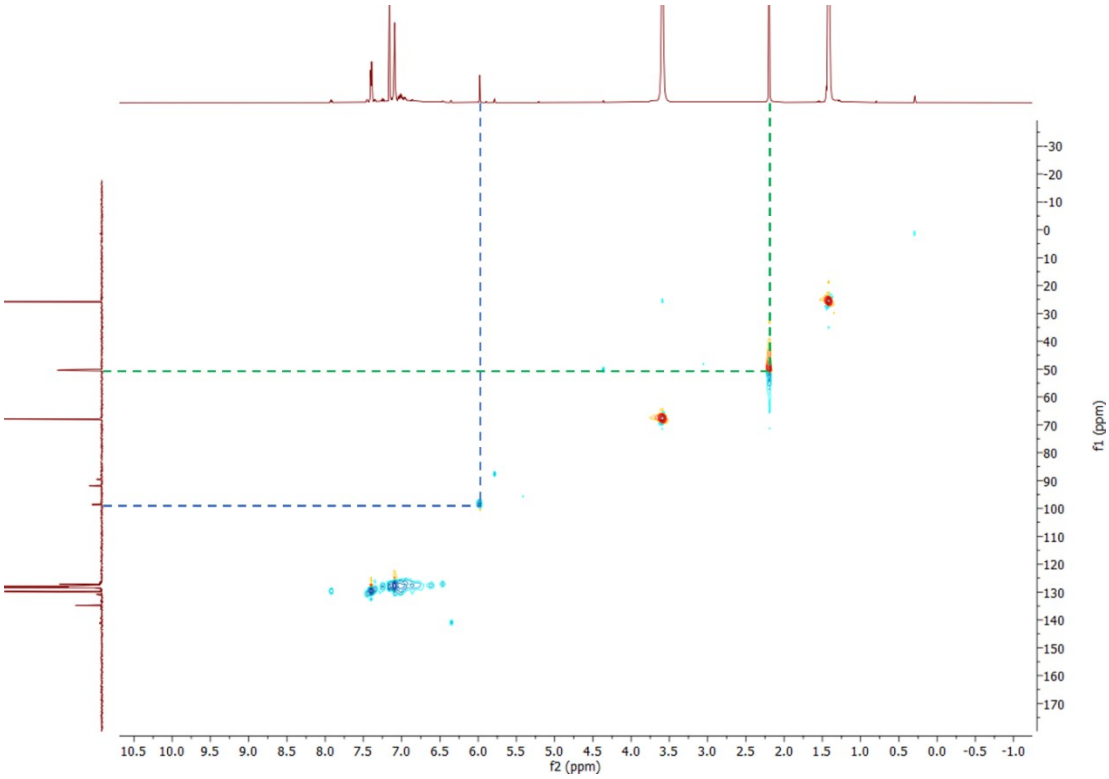

Figure S16: 500 MHz ^{1}H-^{13}C HSQC spectrum of $[Rh^{I}(C_2H_4)_2]_2[\mu:\eta^5:\eta^5Ph_4Pn]$ in C_6D_6 (Blue = H_w, Green = CH_2)

Syn-[Rh^{I}(CO)$_2$]$_2$[μ:η^5:η^5Ph$_4$Pn] (**5**)

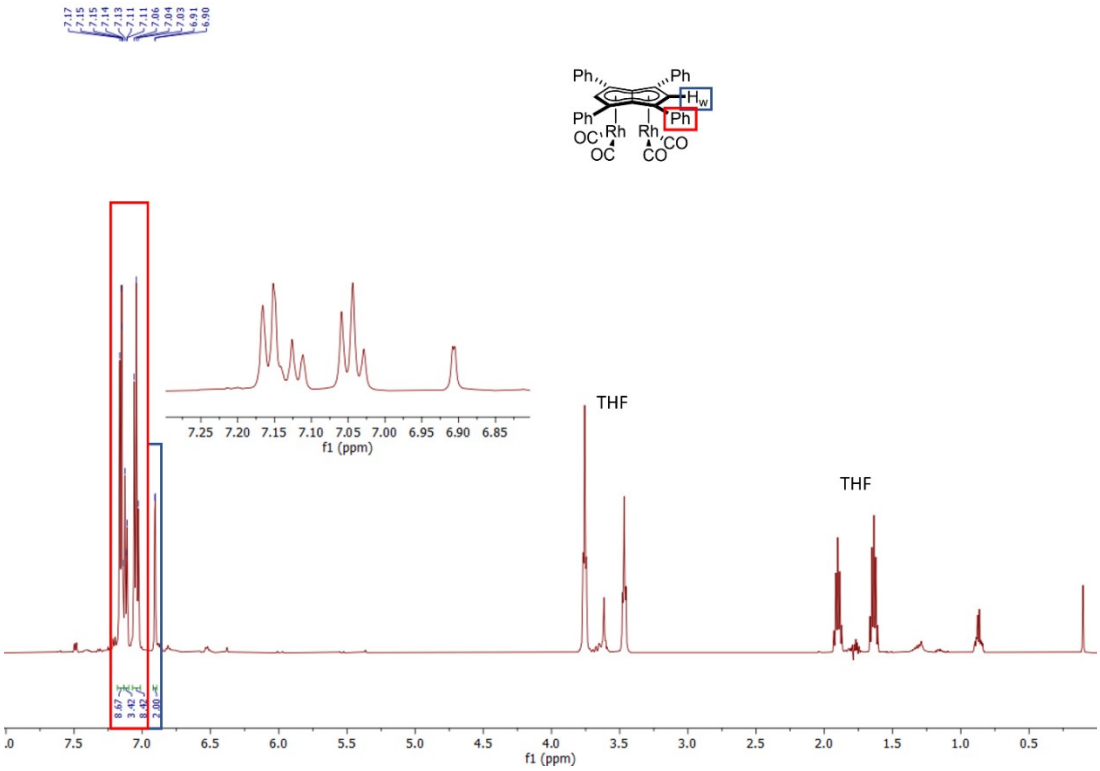

Figure S17: 500 MHz ^{1}H NMR spectrum of [Rh^{I}(CO)$_2$]$_2$[μ:η^5:η^5Ph$_4$Pn] in THF-H$_8$. Spectrum obtained using the lc1gppnf2 solvent suppression pulse sequence, a double presaturation experiment during relaxation and mixing time using two independent channels.

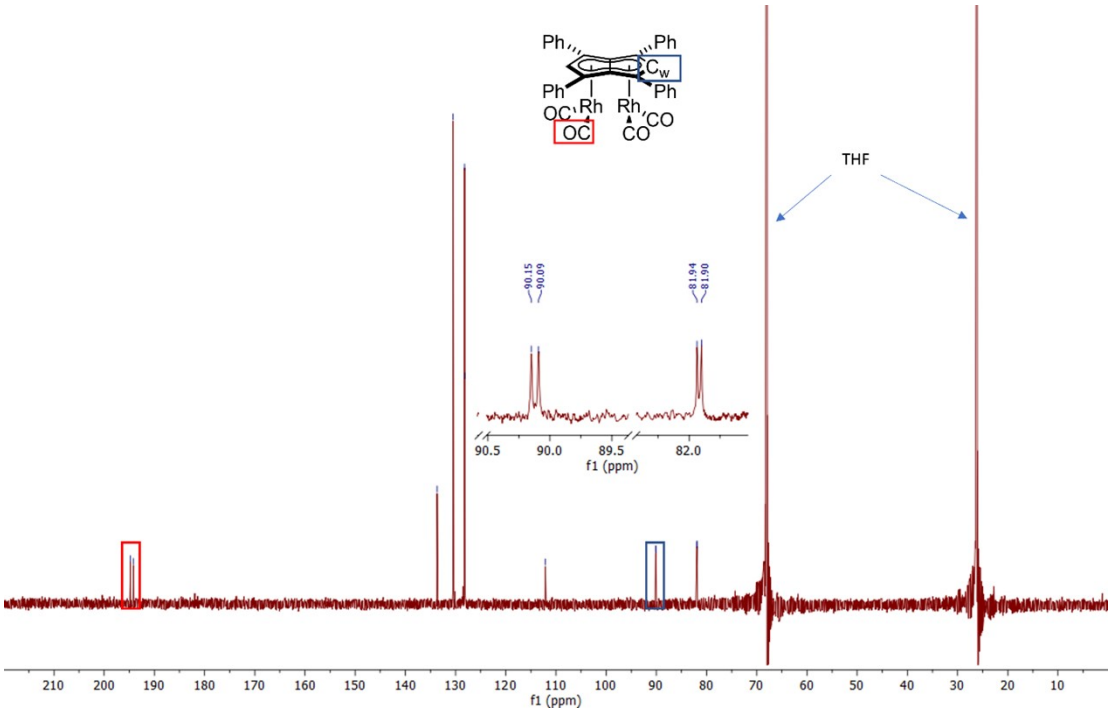

Figure S18: 126 MHz ^{13}C{^{1}H} NMR spectrum of [Rh^{I}(CO)$_2$]$_2$[μ:η^5:η^5Ph$_4$Pn] in THF-H$_8$

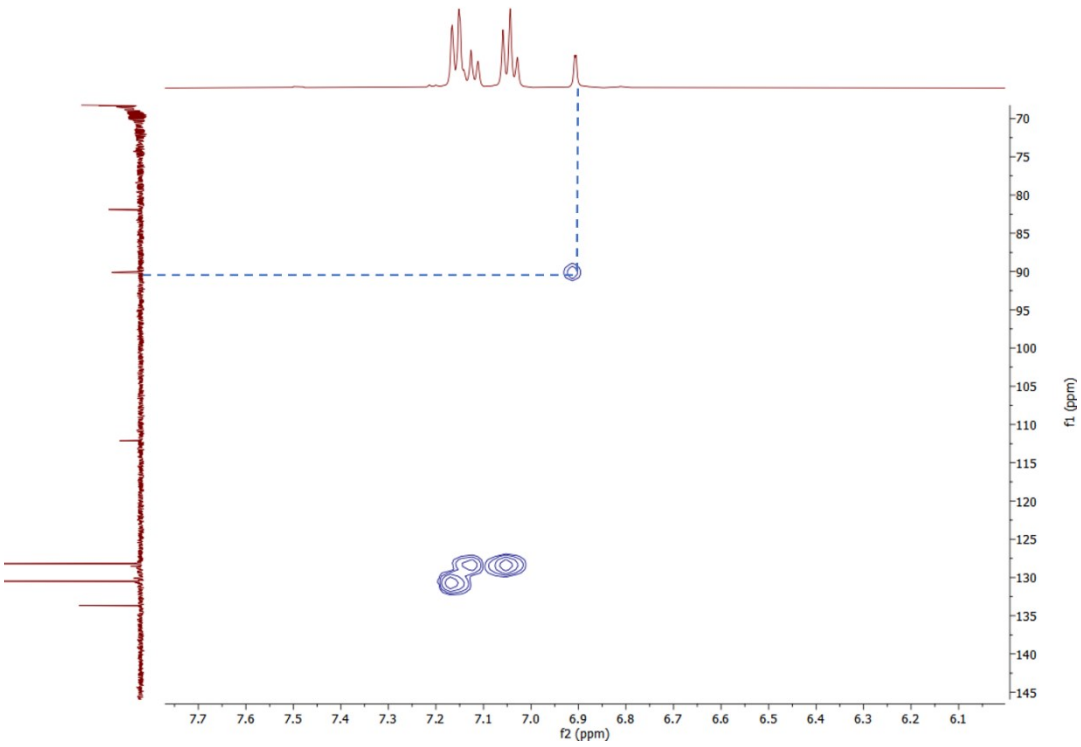

Figure S19: 500 MHz ^{1}H-^{13}C HSQC spectrum of $[Rh^{I}(CO)_2]_2[\mu:\eta^5:\eta^5Ph_4Pn]$ in THF-H_8 (Blue = H_w)

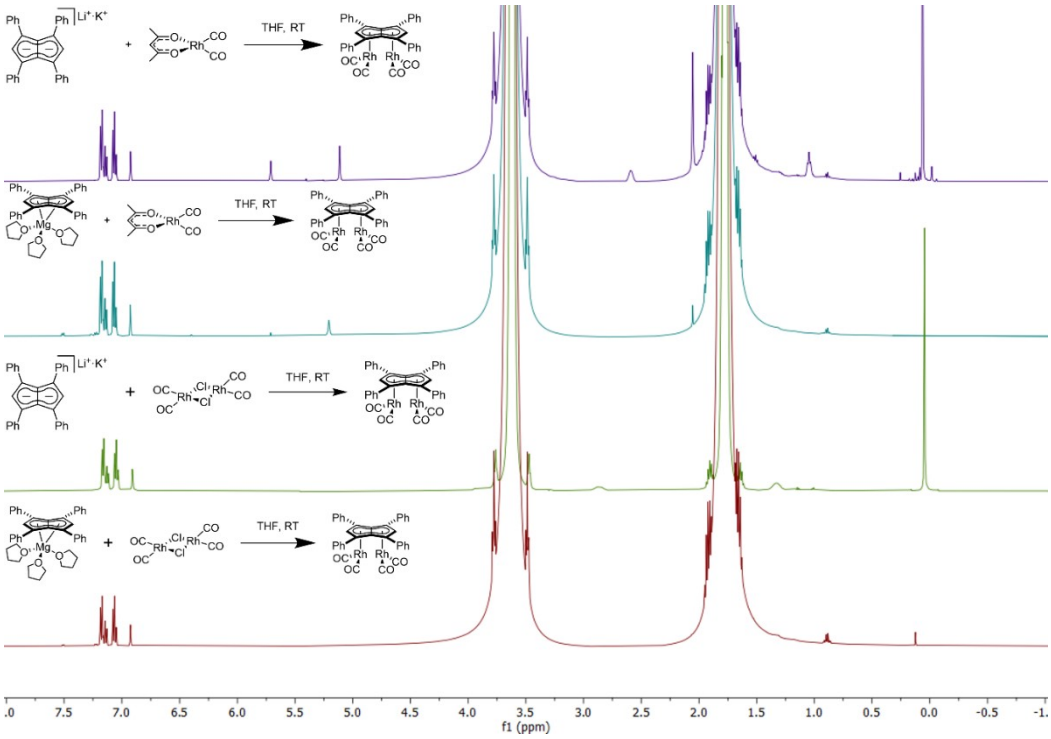

Figure S20: 500 MHz stacked ^{1}H NMR spectra of alternative $[Rh^{I}(CO)_2]_2[\mu:\eta^5:\eta^5Ph_4Pn]$ syntheses in THF-H_8

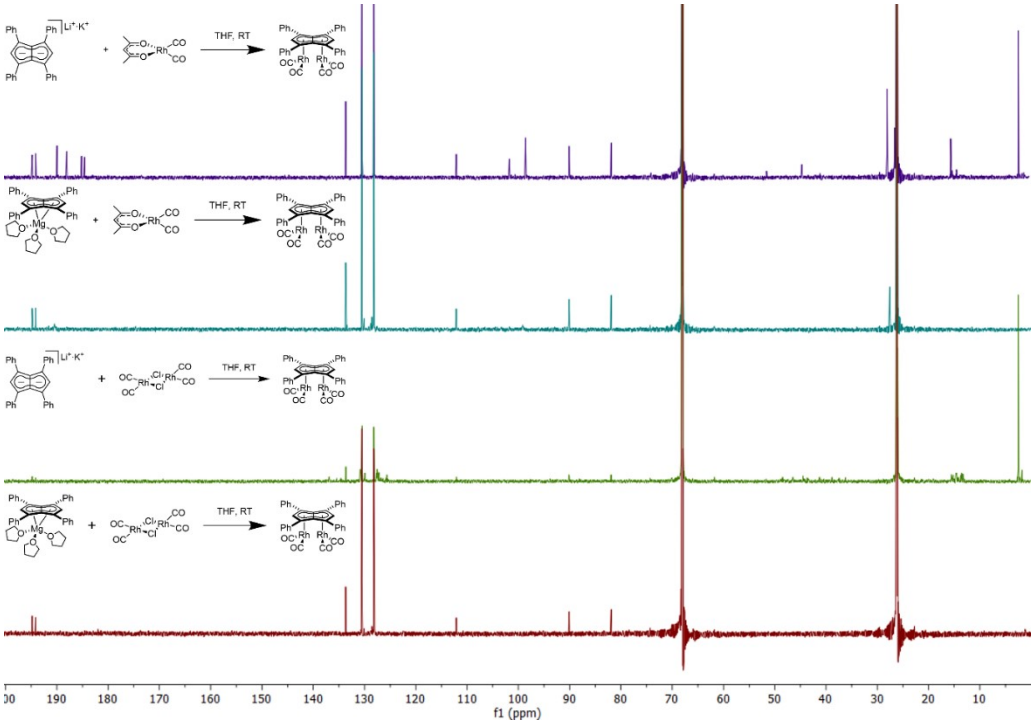

Figure S21: 126 MHz stacked $^{13}C\{^{1}H\}$ NMR spectra of alternative $[Rh^{I}(CO)_2]_2[\mu:\eta^5:\eta^5Ph_4Pn]$ syntheses in THF-H_8

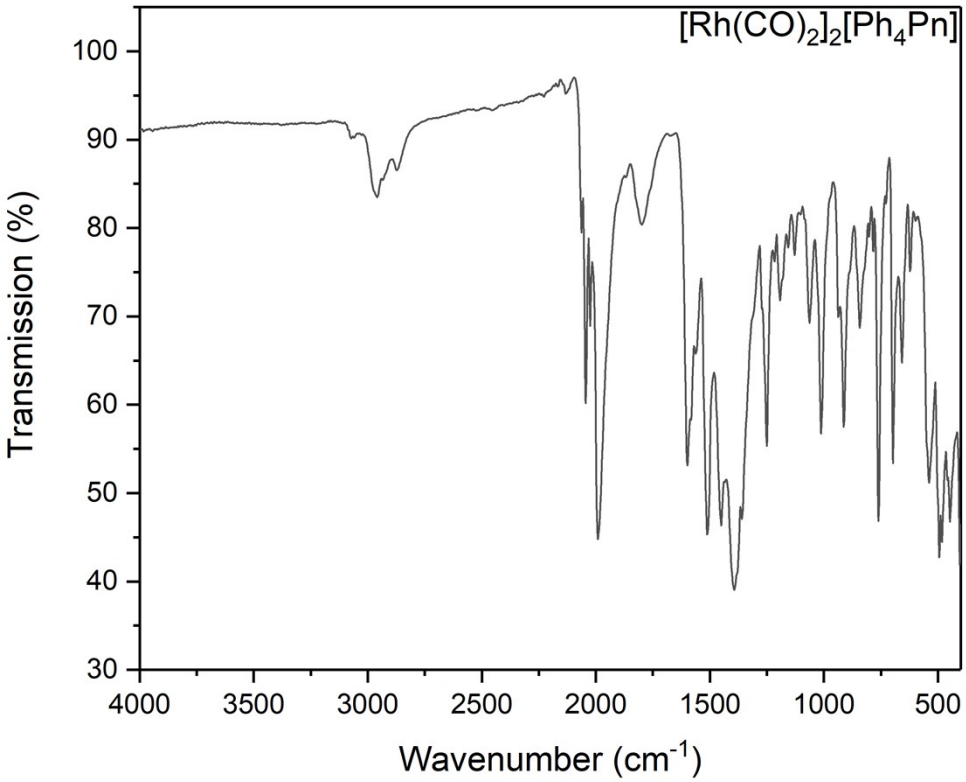

Figure S22: ATR-IR spectrum of solid $[Rh^{I}(CO)_2]_2[\mu:\eta^5:\eta^5Ph_4Pn]$

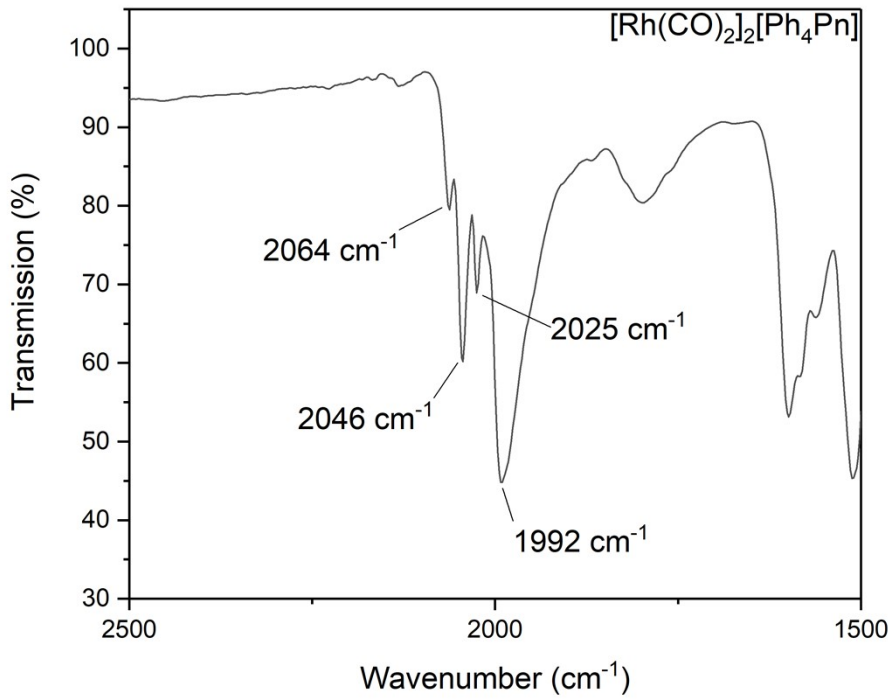

Figure S23: ATR-IR spectrum of solid $[Rh^{I}(CO)_2]_2[\mu{:}\eta^5{:}\eta^5Ph_4Pn]$ (expanded CO region)

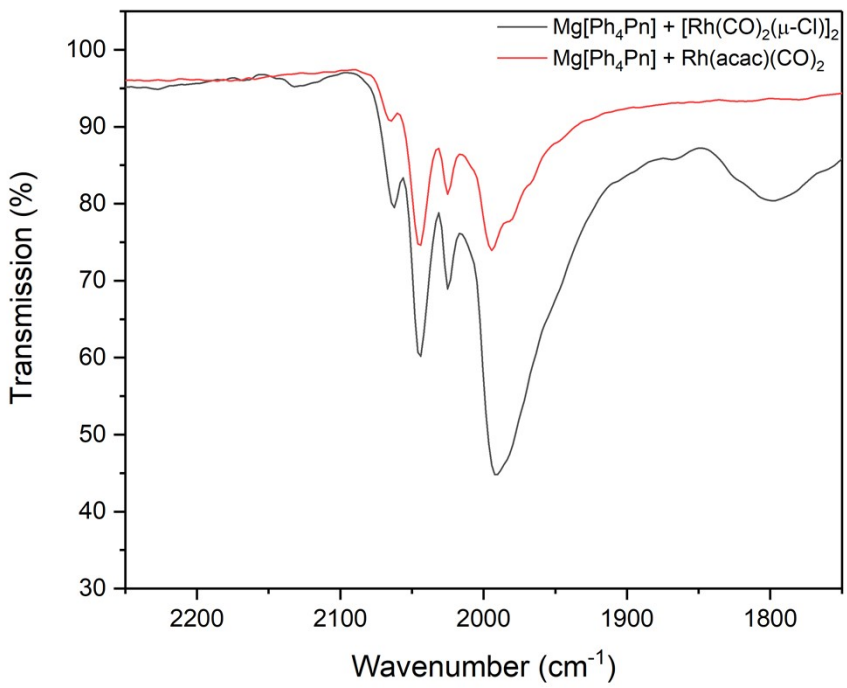

Figure S24: ATR-IR spectra of solid $[Rh^{I}(CO)_2]_2[\mu{:}\eta^5{:}\eta^5Ph_4Pn]$ from alternative syntheses

UV-vis spectra of **1**, **5** and $(Ph_2Cp)Rh^I(CO)_2$

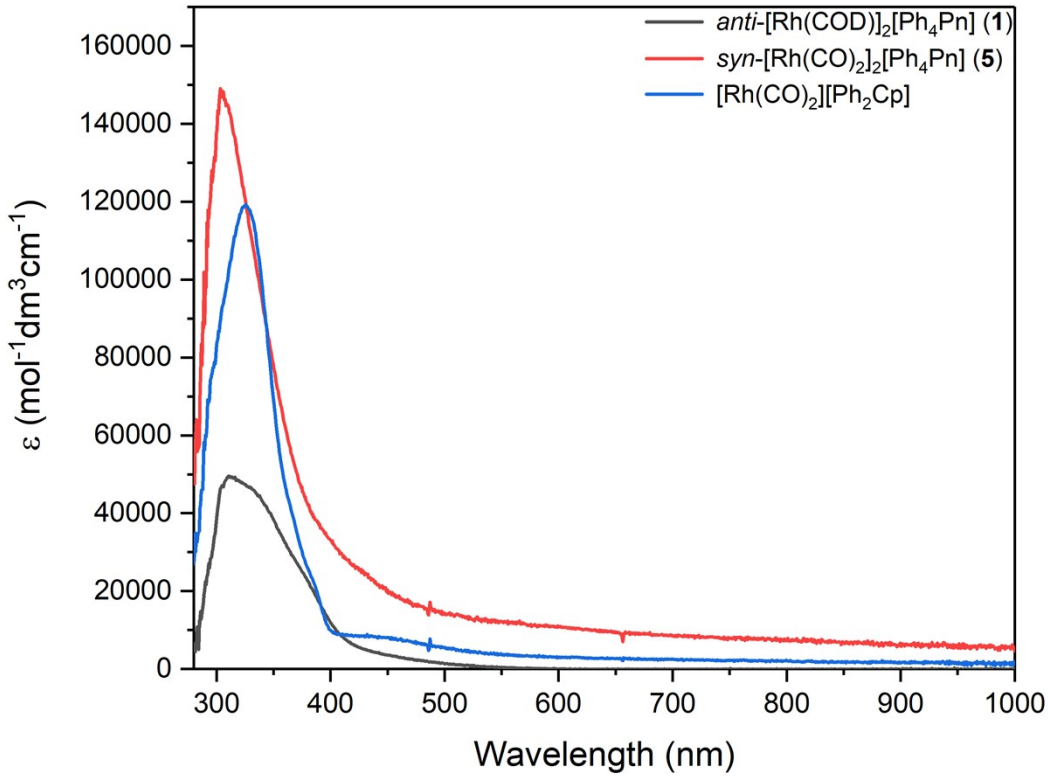

Figure S25: UV-vis spectra of $[Rh^I(COD)]_2[Ph_4Pn]$ (1.5 x 10^{-6} M), $[Rh^I(CO)_2]_2[Ph_4Pn]$ (1.5 x10^{-6} M) and $(Ph_2Cp)Rh^I(CO)_2$ (6.6 x 10^{-6} M)recorded in THF at 298K

Attempted reaction of **5** with 2-2'-bipyridine

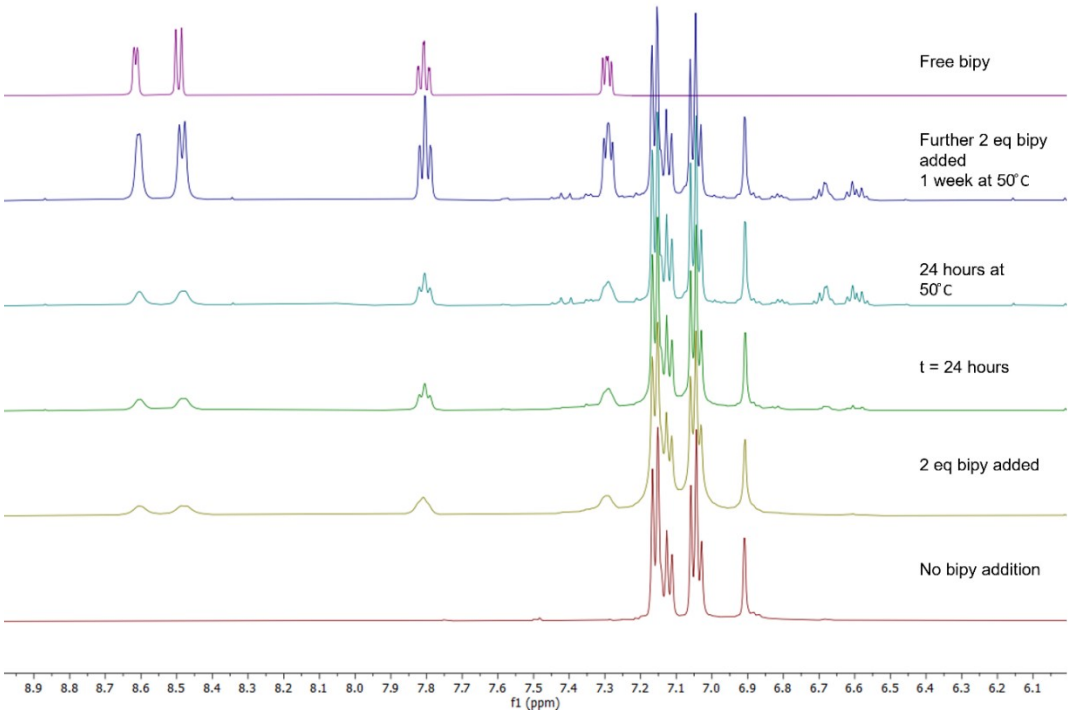

Figure S26: 500 MHz ^{1}H NMR spectra of attempted substitution of $[Rh^I(CO)_2]_2[\mu{:}\eta^5{:}\eta^5Ph_4Pn]$ with 2,2-bipyridine in THF-H_8

Attempted reaction of **5** with pyridine

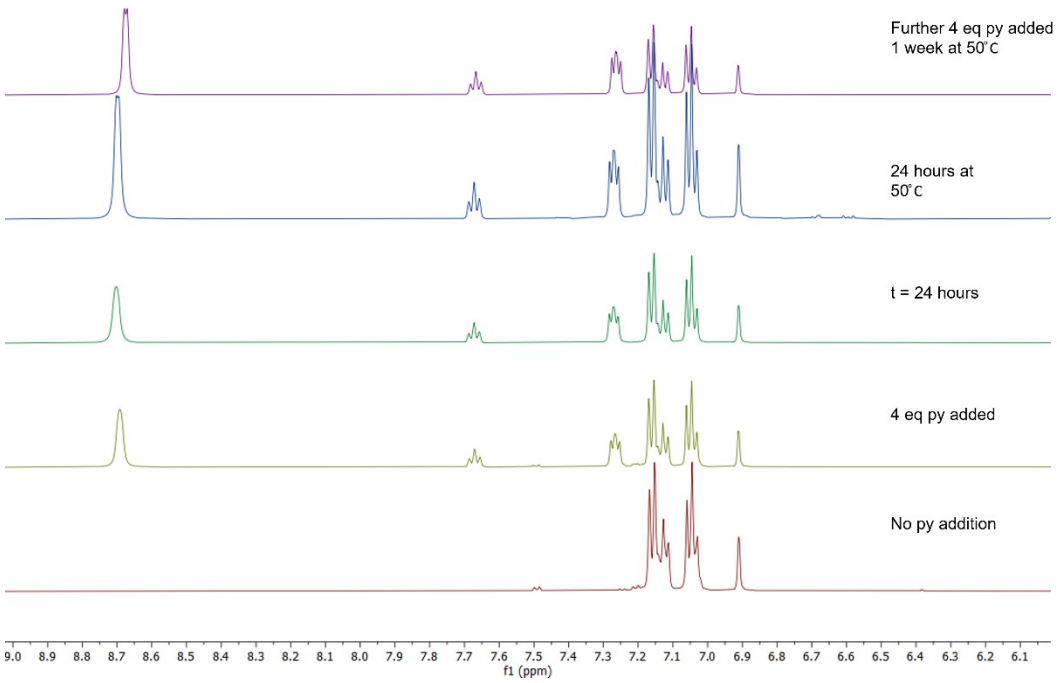

Figure S27: 500 MHz ^{1}H NMR spectra of attempted substitution of $[Rh^I(CO)_2]_2[\mu{:}\eta^5{:}\eta^5Ph_4Pn]$ with pyridine in THF-H_8

Substitution of **5** with Triphenylphosphine

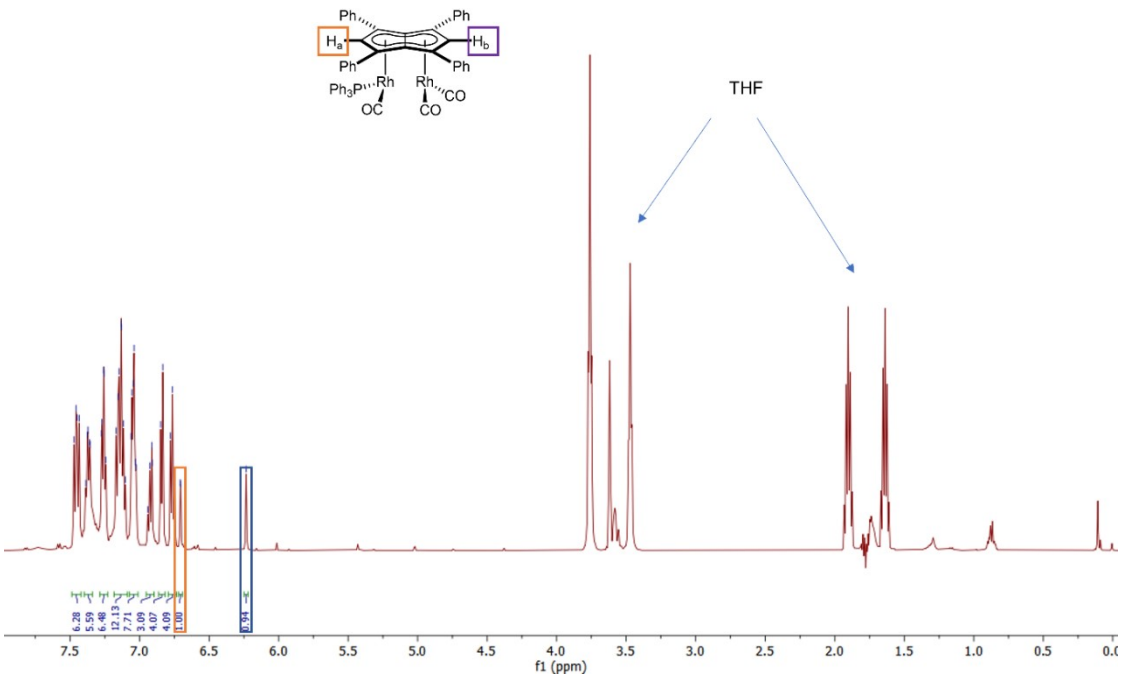

Figure S28: 500 MHz ^{1}H NMR spectrum of *in-situ* formed [Rh^{I}(CO)$_2$Rh(CO)(PPh$_3$)][μ:η^5:η^5Ph$_4$Pn] in THF-H$_8$. Spectrum obtained using the lc1gppnf2 solvent suppression pulse sequence, a double presaturation experiment during relaxation and mixing time using two independent channels.

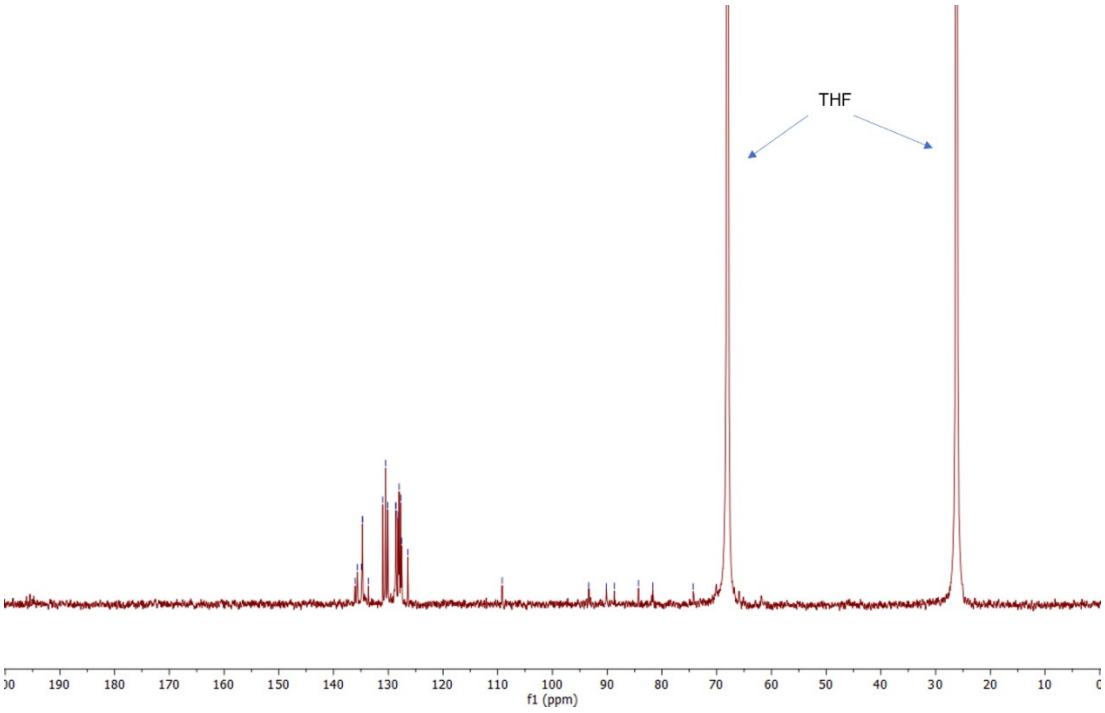

Figure S29: 126 MHz ^{13}C{^{1}H} NMR spectrum of *in-situ* formed [Rh^{I}(CO)$_2$;Rh^{I}(CO)(PPh$_3$)][μ:η^5:η^5Ph$_4$Pn] in THF-H$_8$

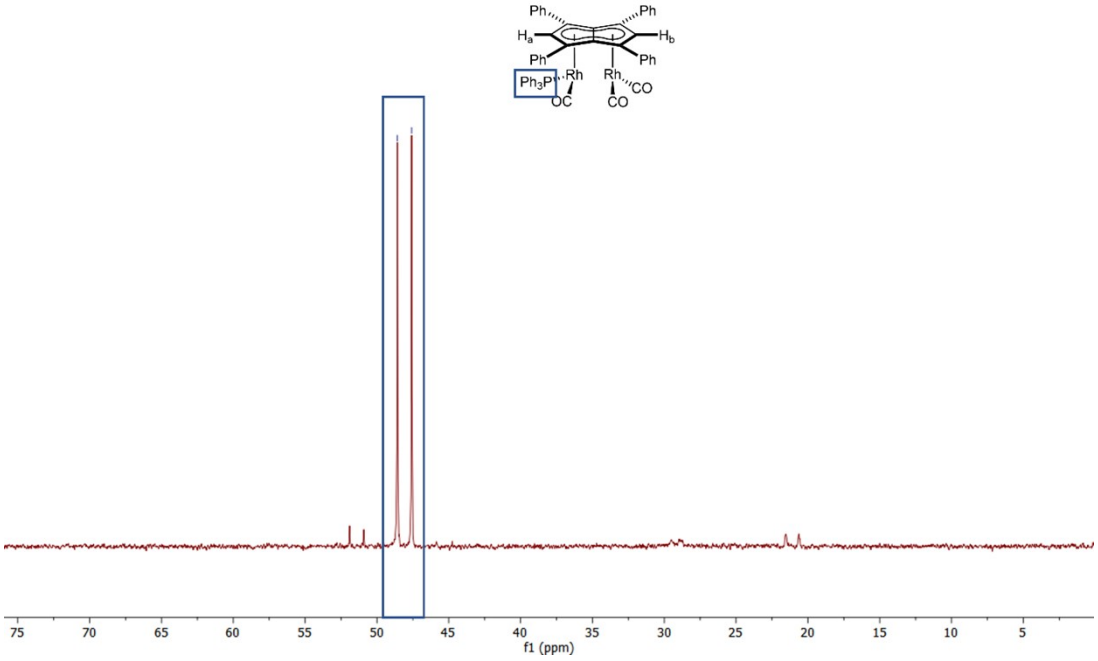

Figure S30: 202 MHz $^{31}P\{^{1}H\}$ NMR spectrum of *in-situ* formed $[Rh^{I}(CO)_2;Rh^{I}(CO)(PPh_3)][\mu:\eta^5:\eta^5Ph_4Pn]$ in THF-H_8

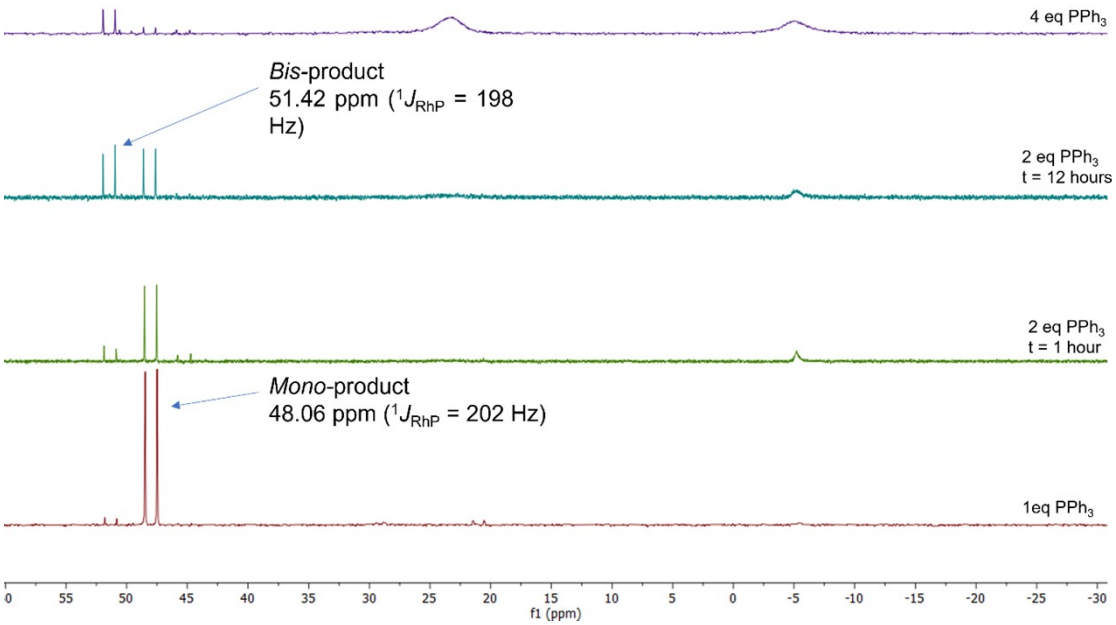

Figure S31: 202 MHz $^{31}P\{^{1}H\}$ NMR spectra of varying equivalents of PPh_3 added to $[Rh^{I}(CO)_2]_2[\mu:\eta^5:\eta^5Ph_4Pn]$ in THF-H_8

Substitution of **5** with Trimethylphosphine

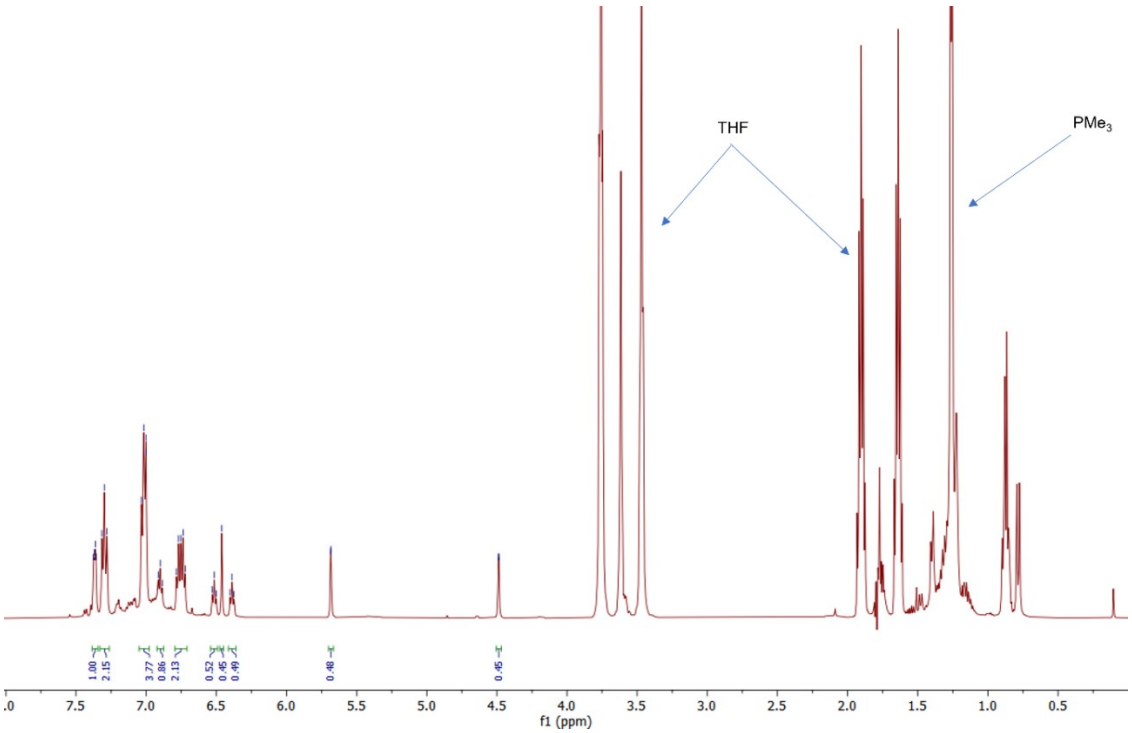

Figure S32: 500 MHz ^{1}H NMR spectrum of four equivalents PMe_3 added to $[Rh^I(CO)_2]_2[\mu{:}\eta^5{:}\eta^5Ph_4Pn]$ in THF-H_8. Spectrum obtained using the lc1gppnf2 solvent suppression pulse sequence, a double presaturation experiment during relaxation and mixing time using two independent channels.

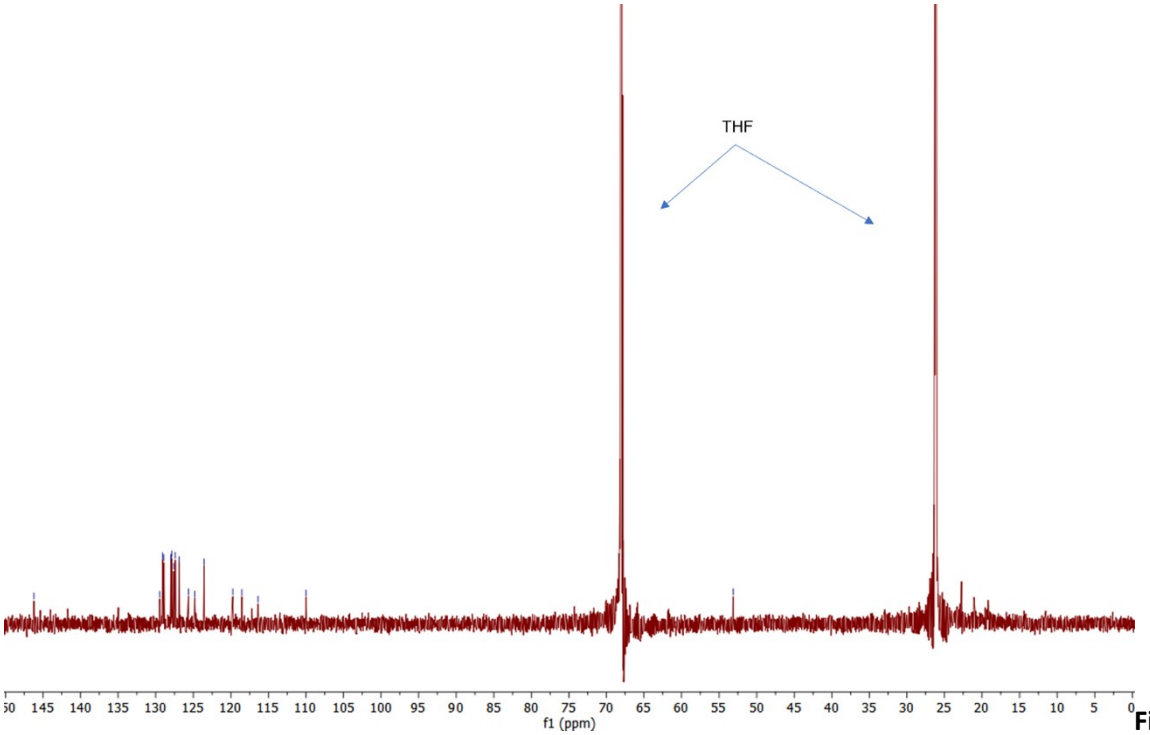

Figure S33: 126 MHz $^{13}C\{^{1}H\}$ NMR spectrum of four equivalents PMe_3 added to $[Rh^{I}(CO)_2]_2[\mu:\eta^5:\eta^5Ph_4Pn]$ in THF-H_8

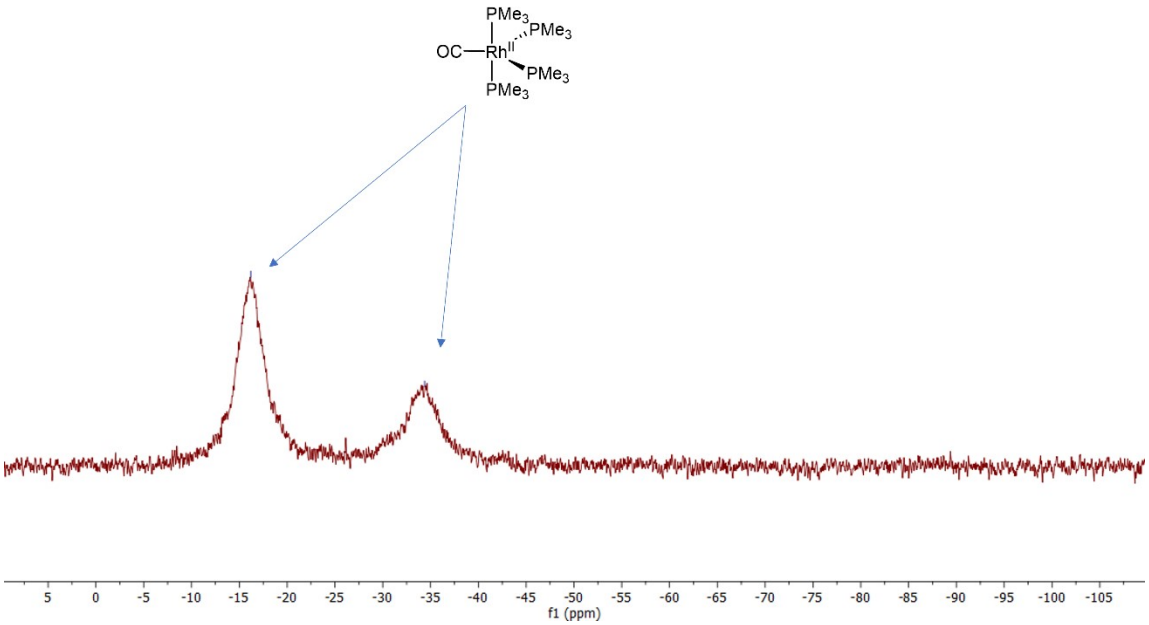

Figure S34: 202 MHz $^{31}P\{^{1}H\}$ NMR spectrum of four equivalents PMe_3 added to $[Rh^{I}(CO)_2]_2[\mu:\eta^5:\eta^5Ph_4Pn]$ in THF-H_8

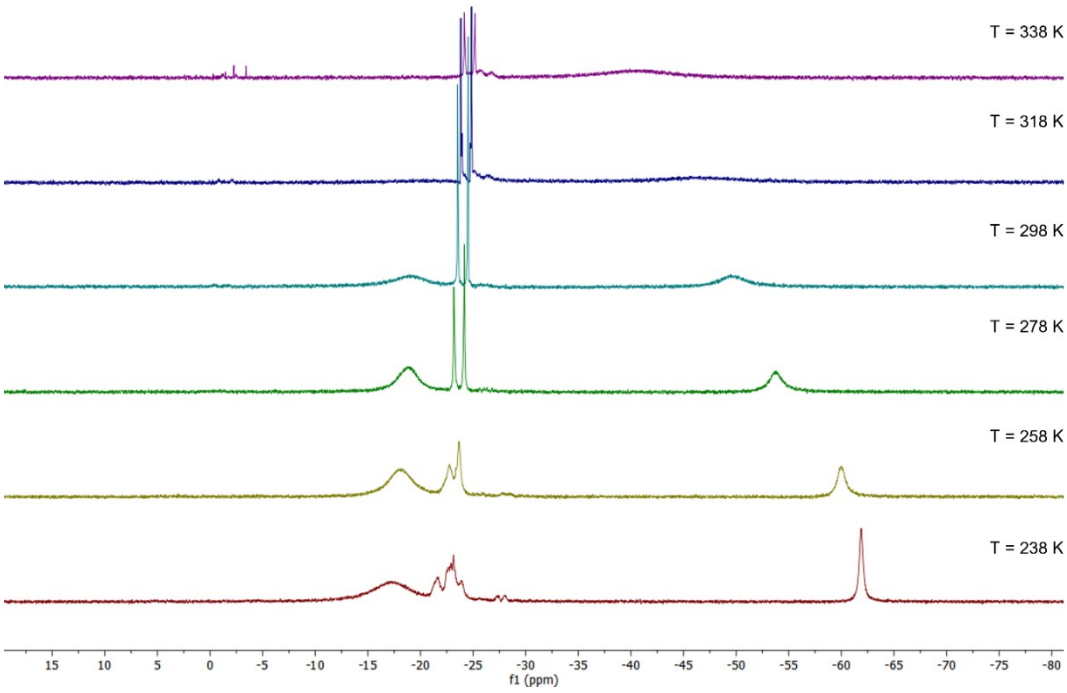

Figure S35: 162 MHz $^{31}P\{^{1}H\}$ variable temperature NMR spectra of four equivalents PMe_3 added to $[Rh^{I}(CO)_2]_2[\mu:\eta^5:\eta^5Ph_4Pn]$ in THF-H_8

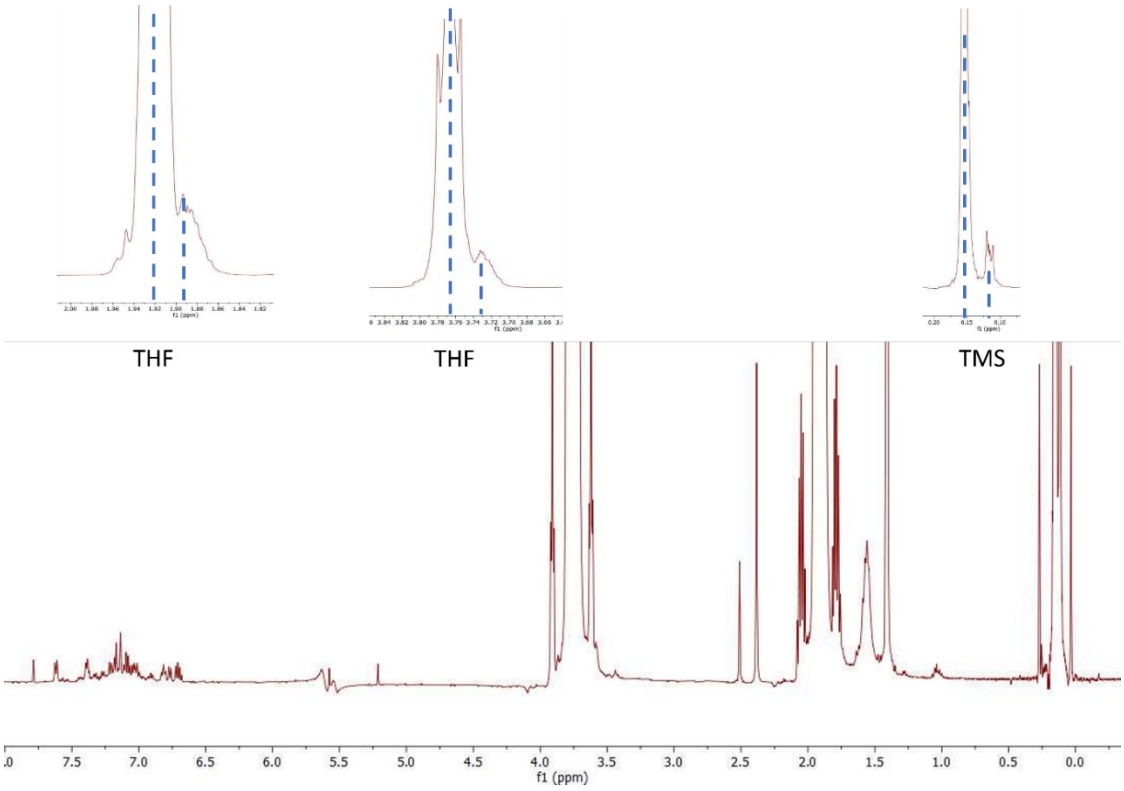

Figure S36: 500 MHz ^{1}H NMR spectrum of four equivalents PMe_3 added to $[Rh^{I}(CO)_2]_2[\mu:\eta^5:\eta^5Ph_4Pn]$ in THF-H_8 with capillary insert of TMS in THF.

Substitution of **5** with bis(diphenylphosphino)ethane

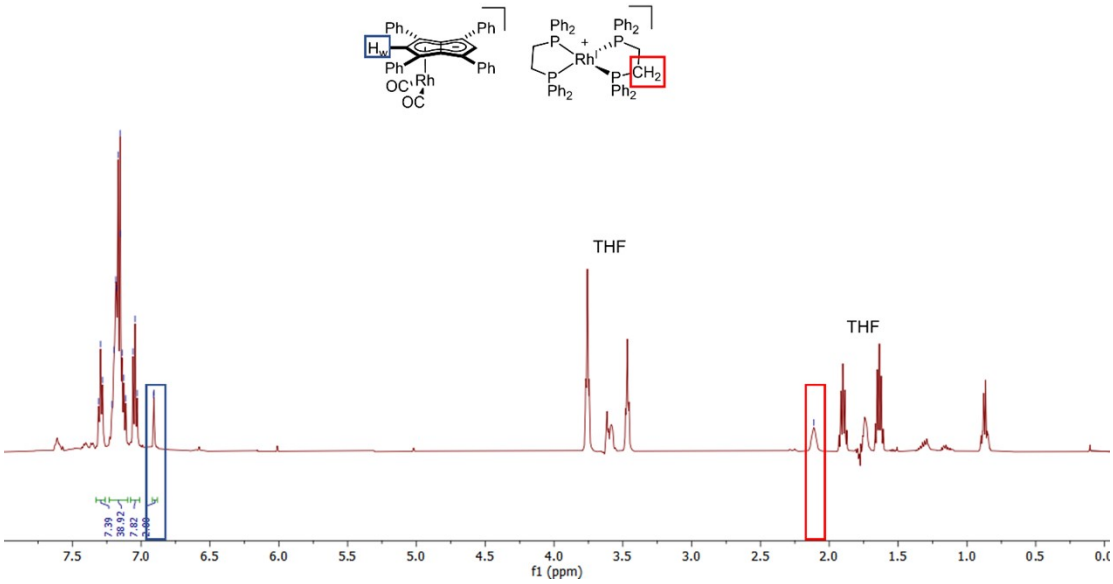

Figure S37: 500 MHz ^{1}H NMR spectrum of *in-situ* formed [Rh^{I}(dppe)$_2$][Rh(CO)$_2$(η^5Ph$_4$Pn)] in THF-H$_8$. Spectrum obtained using the lc1gppnf2 solvent suppression pulse sequence, a double presaturation experiment during relaxation and mixing time using two independent channels.

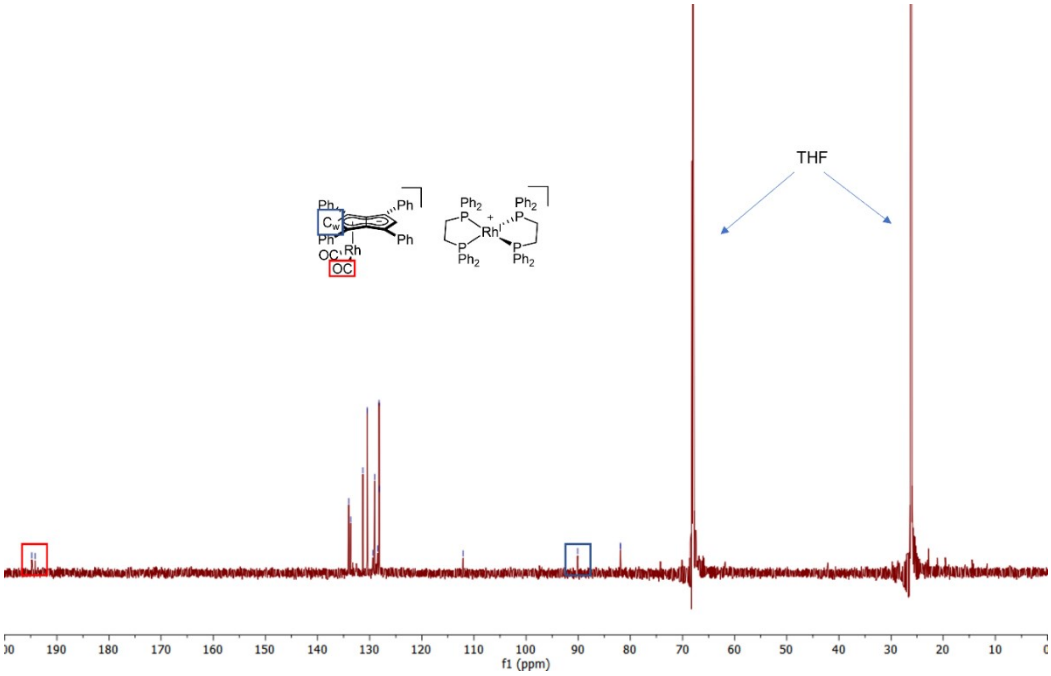

Figure S38: 126 MHz ^{13}C{^{1}H} NMR spectrum of *in-situ* formed [Rh^{I}(dppe)$_2$][Rh^{I}(CO)$_2$(η^5Ph$_4$Pn)] in THF-H$_8$

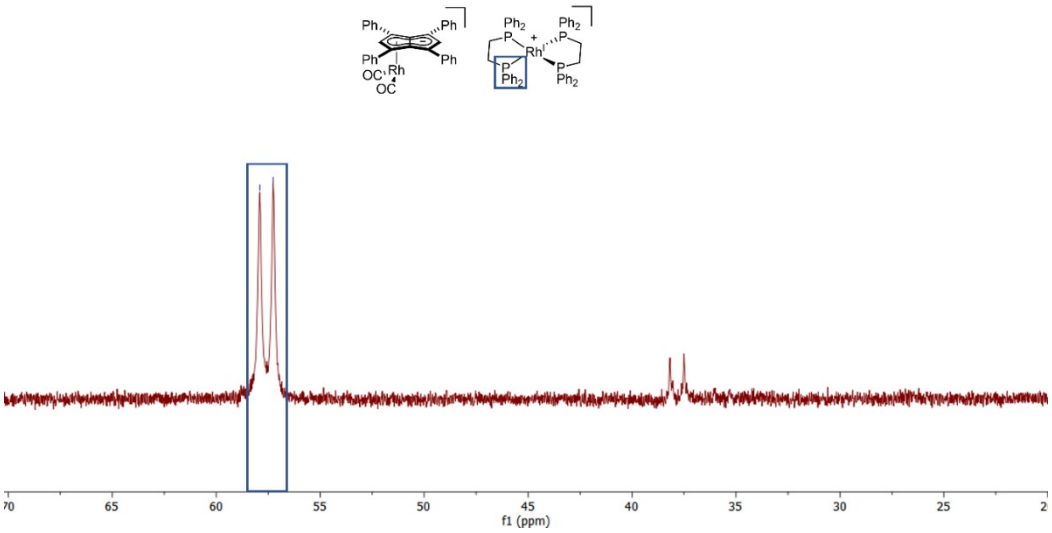

Figure S39: 202 MHz $^{31}P\{^{1}H\}$ NMR spectrum of *in-situ* formed $[Rh^{I}(dppe)_2][Rh^{I}(CO)_2(\eta^5Ph_4Pn)]$ in THF-H_8

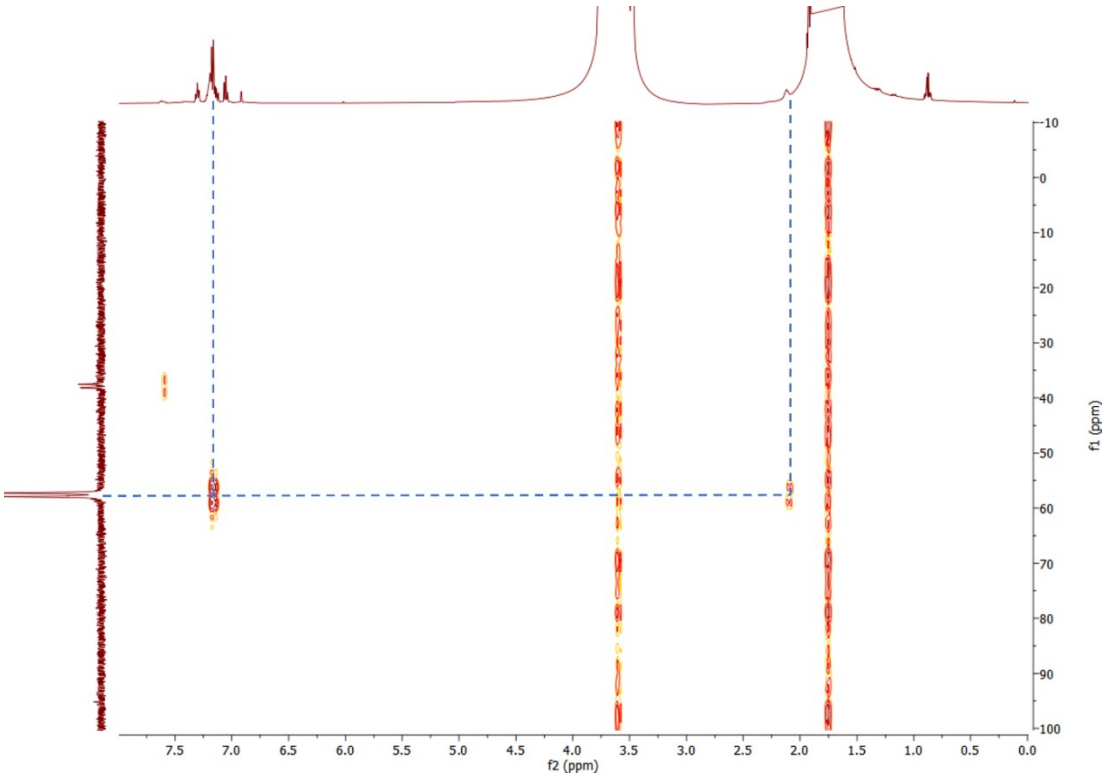

Figure S40: 500 MHz ^{1}H-^{31}P HMBC spectrum of *in-situ* formed $[Rh(dppe)_2][Rh(CO)_2(\eta^5Ph_4Pn)]$ in THF-H_8 (Blue = $Rh(dppe)_2^+$)

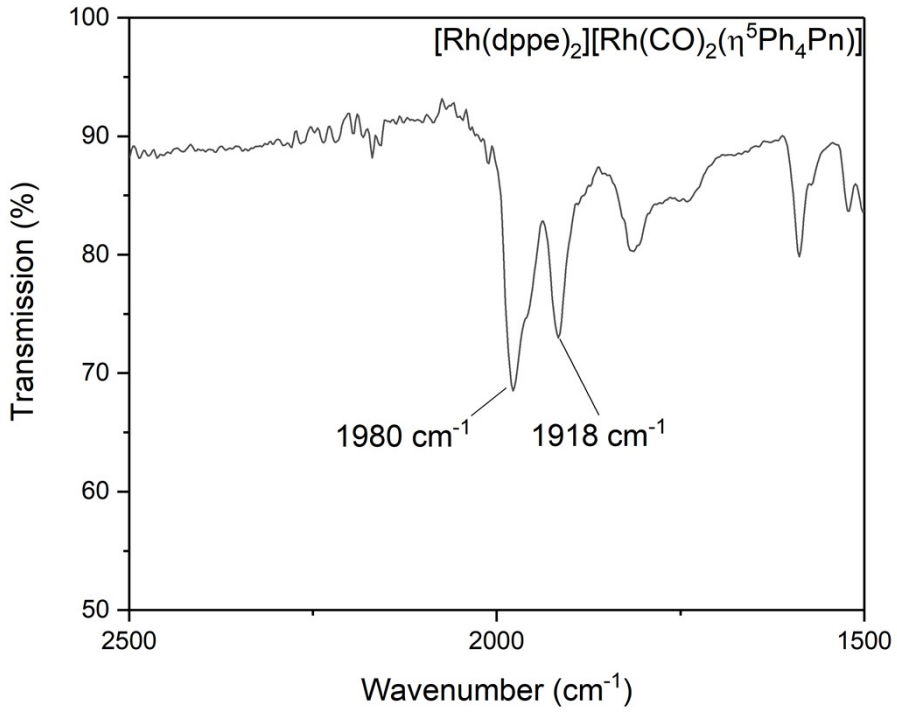

Figure S41: ATR-IR spectrum of solid $[Rh^{I}(dppe)_2][Rh^{I}(CO)_2(\eta^5Ph_4Pn)]$ (expanded CO region)

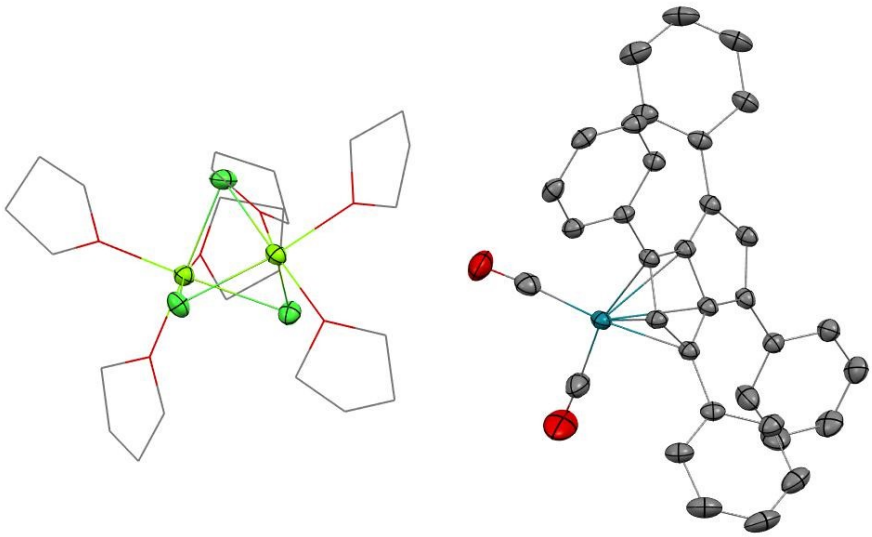

Figure S42: XRD structure of $[Mg_2(\mu\text{-}Cl)_3(THF)_6[Rh^{I}(CO)_2(\eta^5\text{-}Ph_4Pn]$ with thermal ellipsoids at the 50% probability level (hydrogens omitted for clarity)

Reaction of **5** with Triphenylphosphite

1eq P(OPh)$_3$

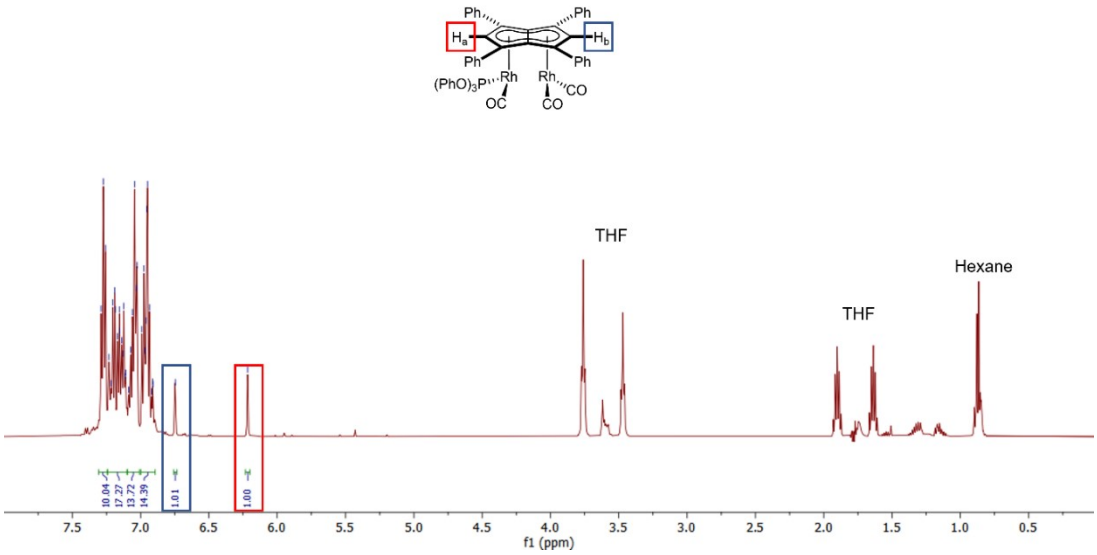

Figure S43: 500 MHz ^{1}H NMR spectrum of *in-situ* [Rh^I(CO)$_2$;Rh^I(CO)(P{OPh}$_3$)][μ:η^5:η^5Ph$_4$Pn] in THF-H$_8$. Spectrum obtained using the lc1gppnf2 solvent suppression pulse sequence, a double presaturation experiment during relaxation and mixing time using two independent channels.

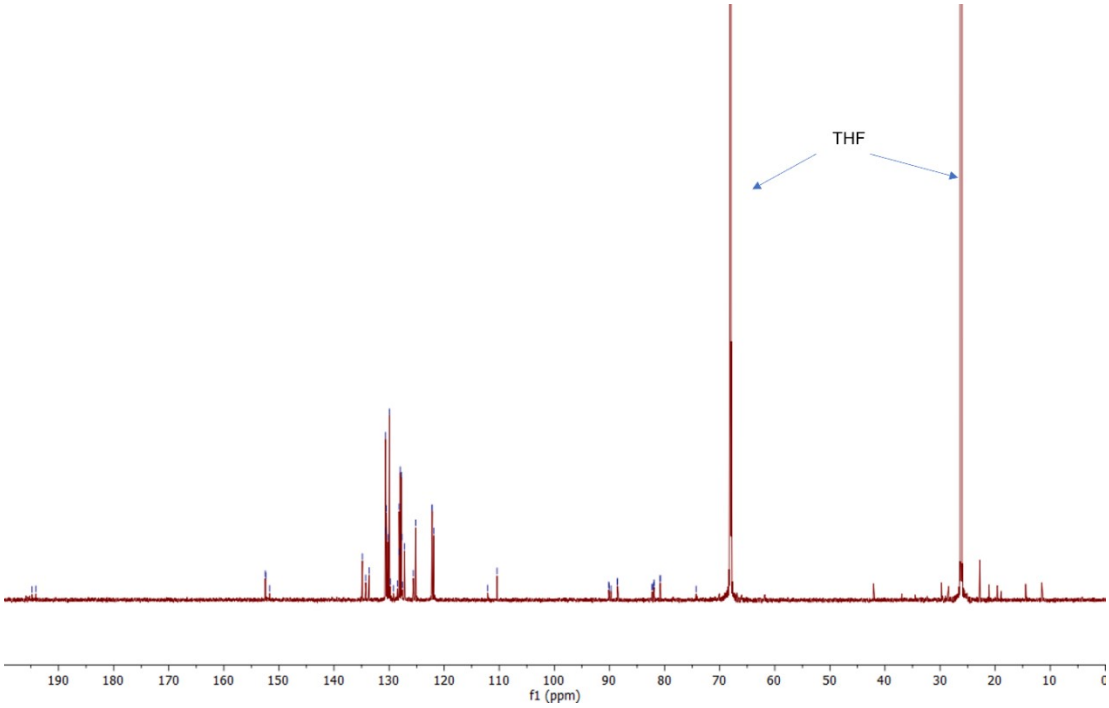

Figure S44: 126 MHz ^{13}C{^{1}H} NMR spectrum of *in-situ* [Rh^I(CO)$_2$;Rh^I(CO)(P{OPh}$_3$)][μ:η^5:η^5Ph$_4$Pn] in THF-H$_8$

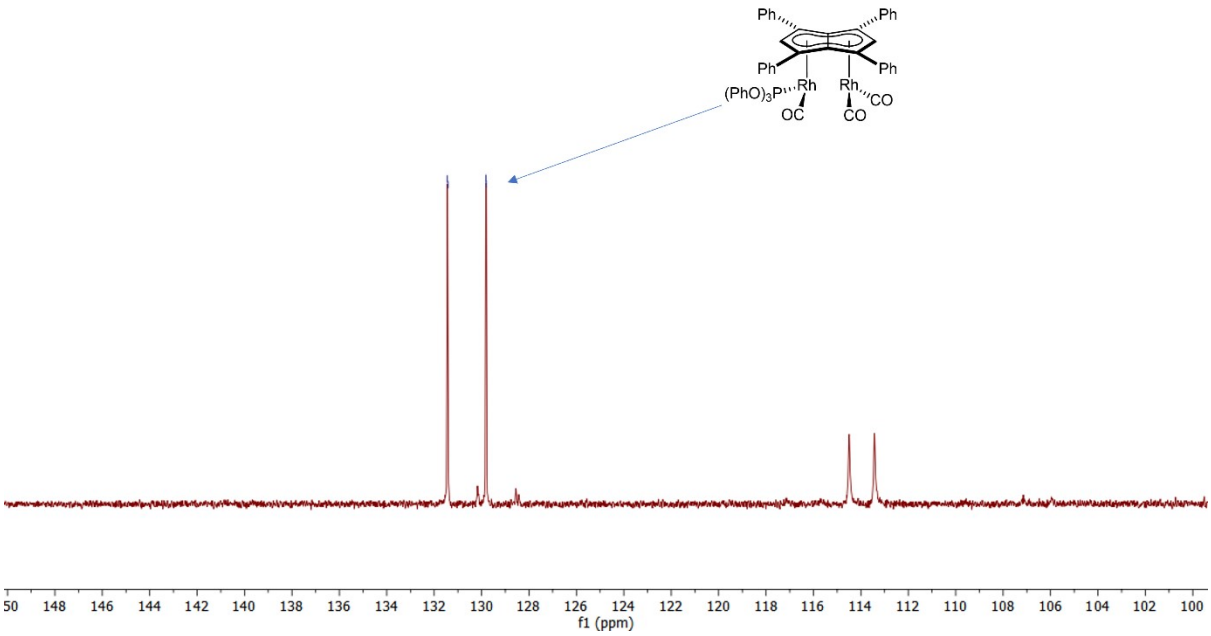

Figure S45: 202 MHz $^{31}P\{^{1}H\}$ NMR spectrum of *in-situ* $[Rh^{I}(CO)_2;Rh^{I}(CO)(P\{OPh\}_3)][\mu:\eta^5:\eta^5Ph_4Pn]$ in THF-H_8

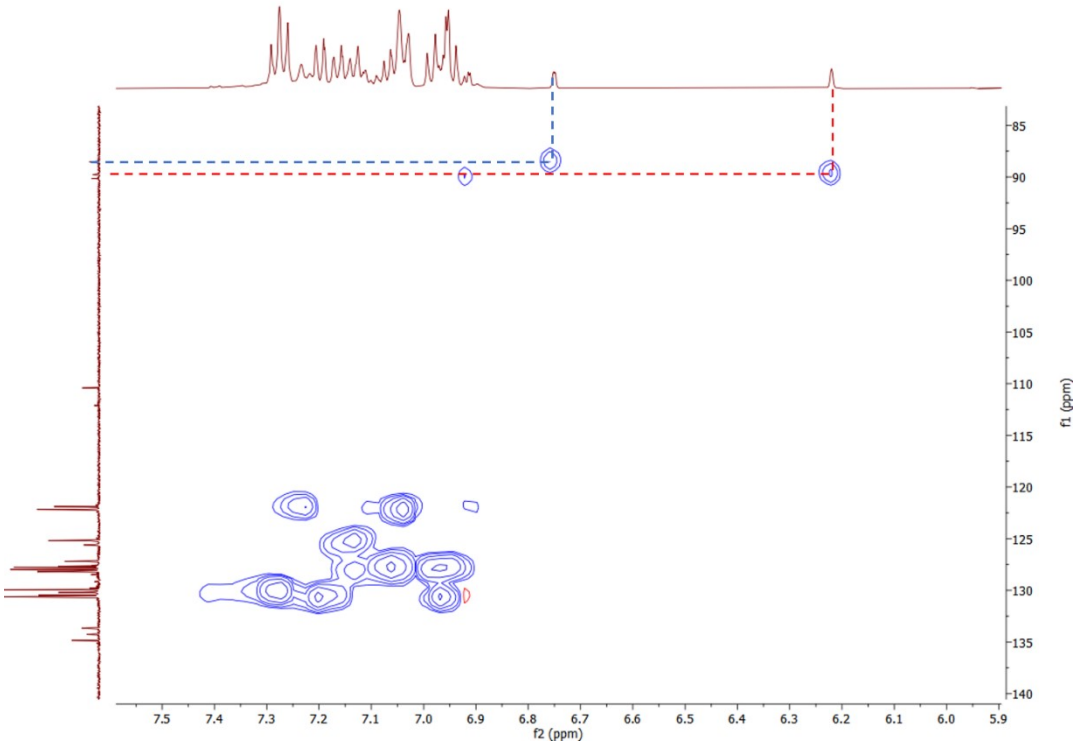

Figure S46: 500 MHz ^{1}H-^{13}C HSQC spectrum of *in-situ* $[Rh^{I}(CO)_2;Rh^{I}(CO)(P\{OPh\}_3)][\mu:\eta^5:\eta^5Ph_4Pn]$in THF-$H_8$ (Blue = H_b, Red = H_a)

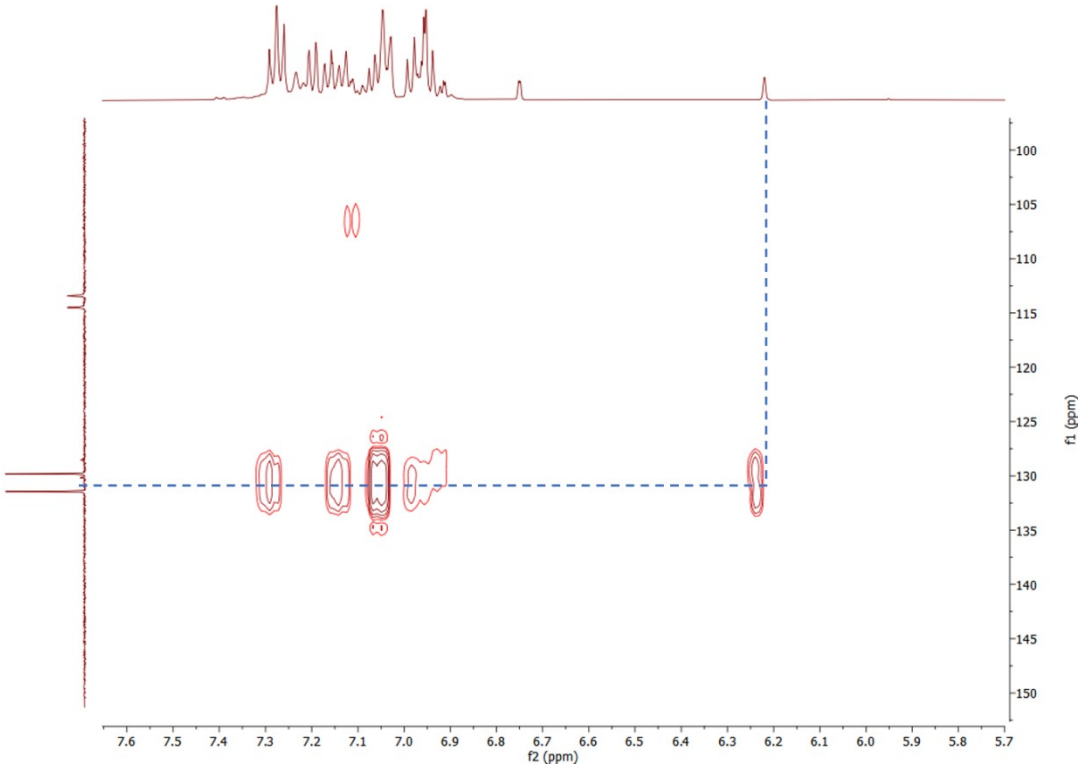

Figure S47: 500 MHz ^{1}H-^{31}P HMBC spectrum of *in-situ* $[Rh^{I}(CO)_2;Rh^{I}(CO)(P\{OPh\}_3)][\mu:\eta^5:\eta^5Ph_4Pn]$ in THF-H_8 (Blue = H_a)

[Rh^{I}(CO)(P{OPh}$_3$)]$_2$[μ:η^5:η^{5}Ph$_4$Pn] (**11**)

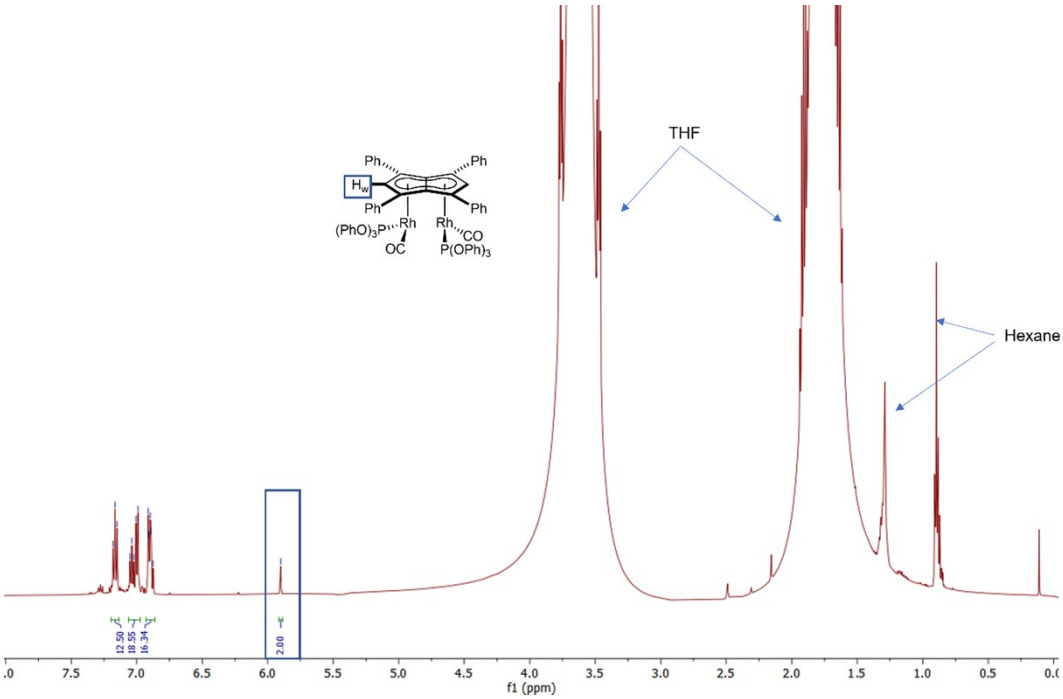

Figure S48: 500 MHz ^{1}H NMR spectrum of [Rh^{I}(CO)(P{OPh}$_3$)]$_2$[μ:η^5:η^5Ph$_4$Pn] in THF-H$_8$

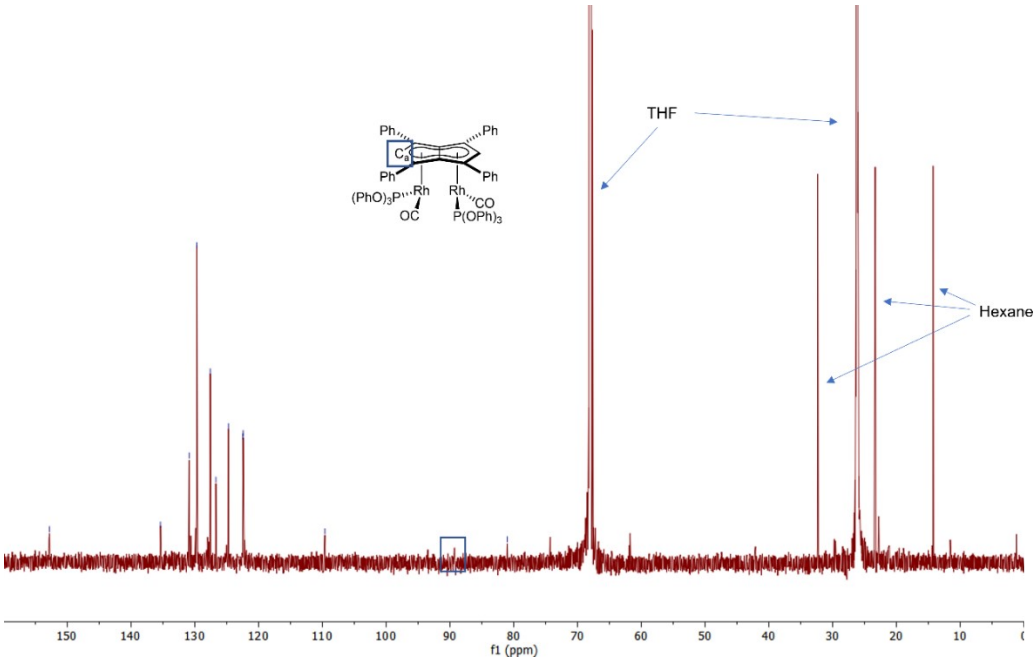

Figure S49: 126 MHz ^{13}C{^{1}H} NMR spectrum of [Rh^{I}(CO)(P{OPh}$_3$)]$_2$[μ:η^5:η^5Ph$_4$Pn] in THF-H$_8$

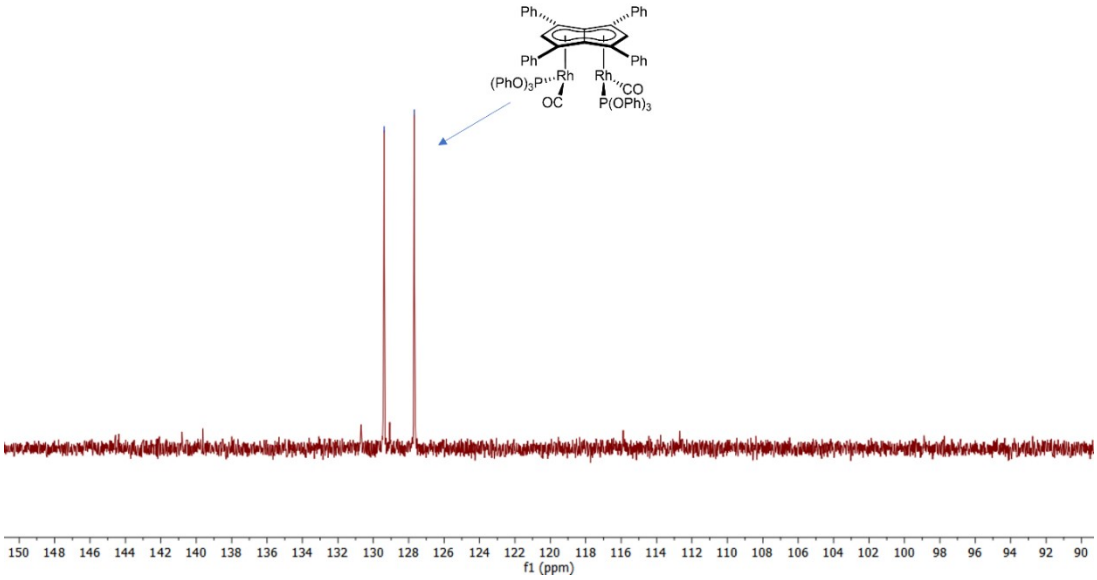

Figure S50: 202 MHz $^{31}P\{^{1}H\}$ NMR spectrum of $[Rh^{I}(CO)(P\{OPh\}_3)]_2[\mu:\eta^5:\eta^5Ph_4Pn]$ in THF-H_8

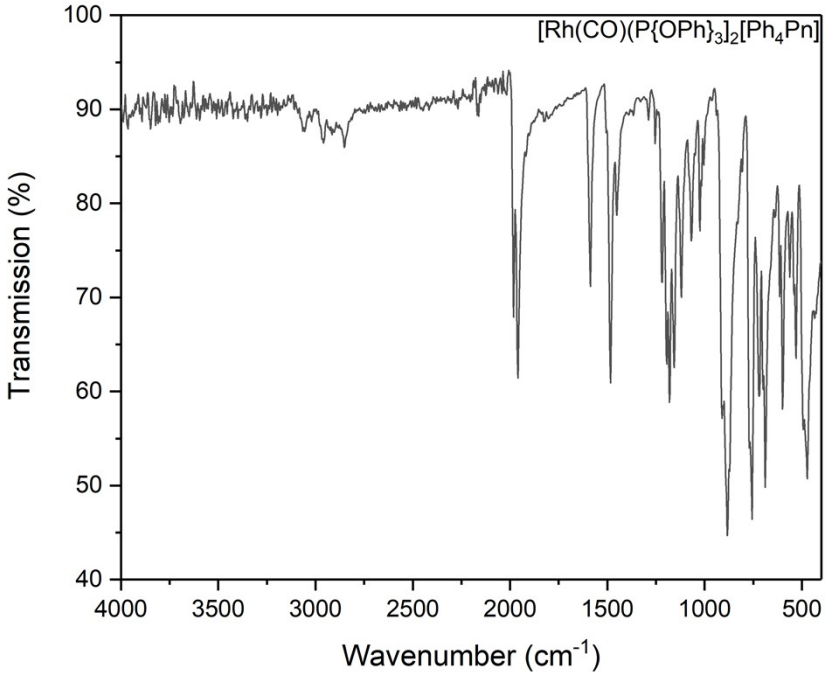

Figure S51: ATR-IR spectrum of solid $[Rh^{I}(CO)(P\{OPh\}_3)]_2[\mu:\eta^5:\eta^5Ph_4Pn]$

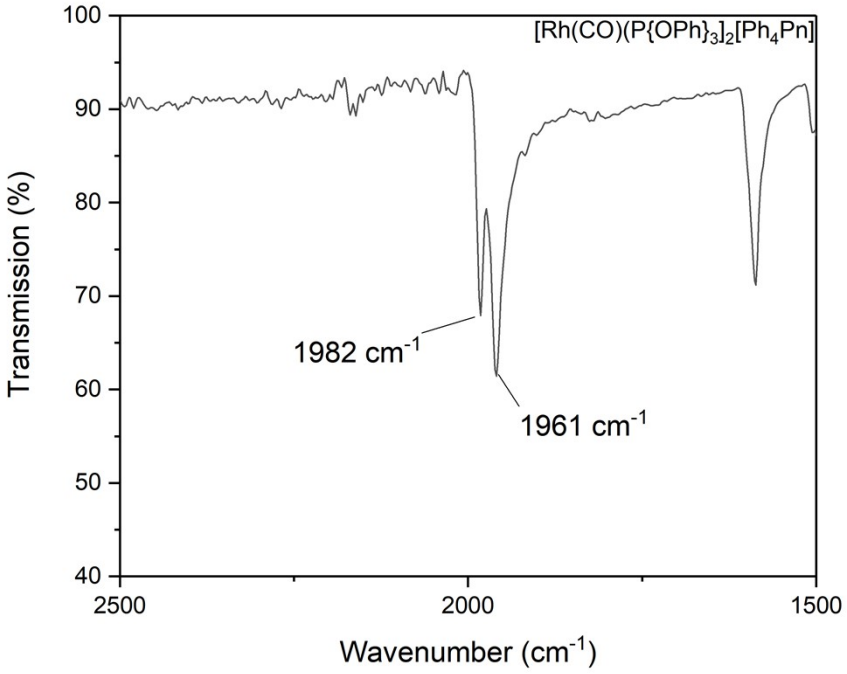

Figure S52: ATR-IR spectrum of solid [Rh^{I}(CO)(P{OPh}$_3$)]$_2$[μ:η^5:η^5Ph$_4$Pn], expansion of CO region.

Reaction of 5 with Trimethylphosphite

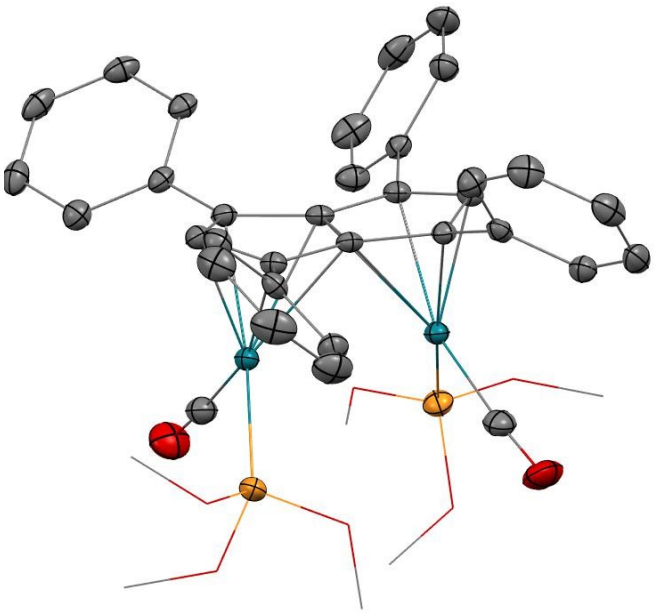

Figure S53: XRD structure of *E-syn*-[Rh^{I}(CO)(P{OMe}$_3$)]$_2$[Ph$_4$Pn] with thermal ellipsoids at the 50% probability level (hydrogens omitted for clarity)

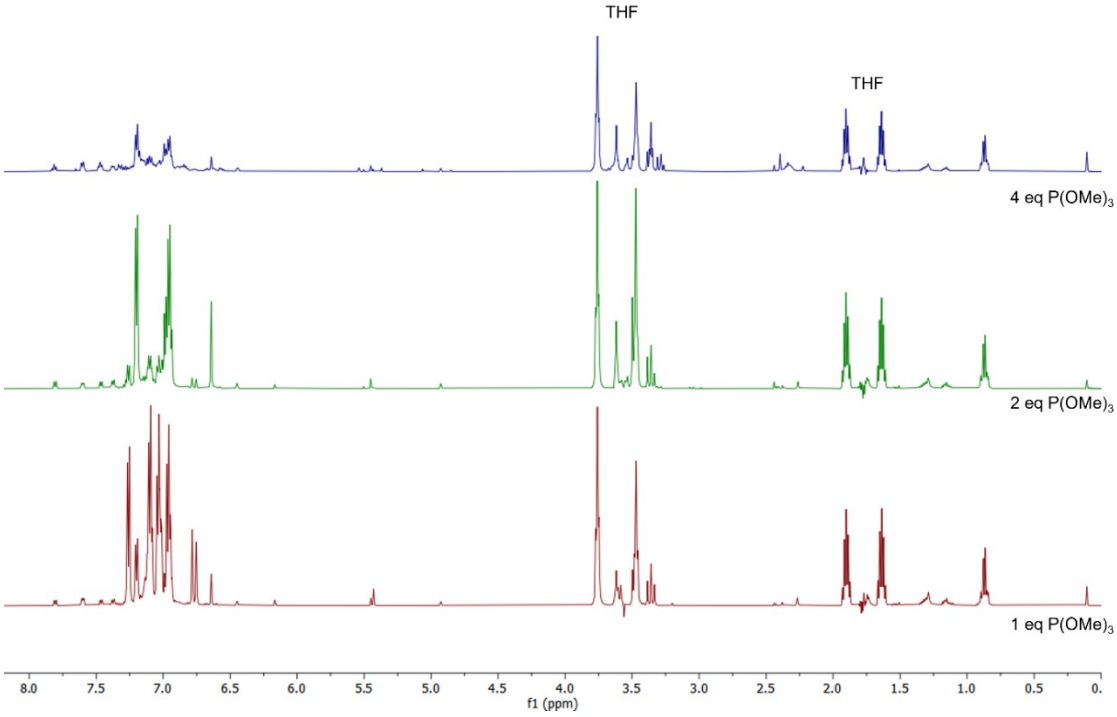

Figure S54: 500 MHz ^{1}H NMR spectra of addition of $P(OMe)_3$ to $[Rh^{I}(CO)_2]_2[\mu:\eta^5:\eta^5Ph_4Pn]$ in THF-H_8. Spectra obtained using the lc1gppnf2 solvent suppression pulse sequence, a double presaturation experiment during relaxation and mixing time using two independent channels.

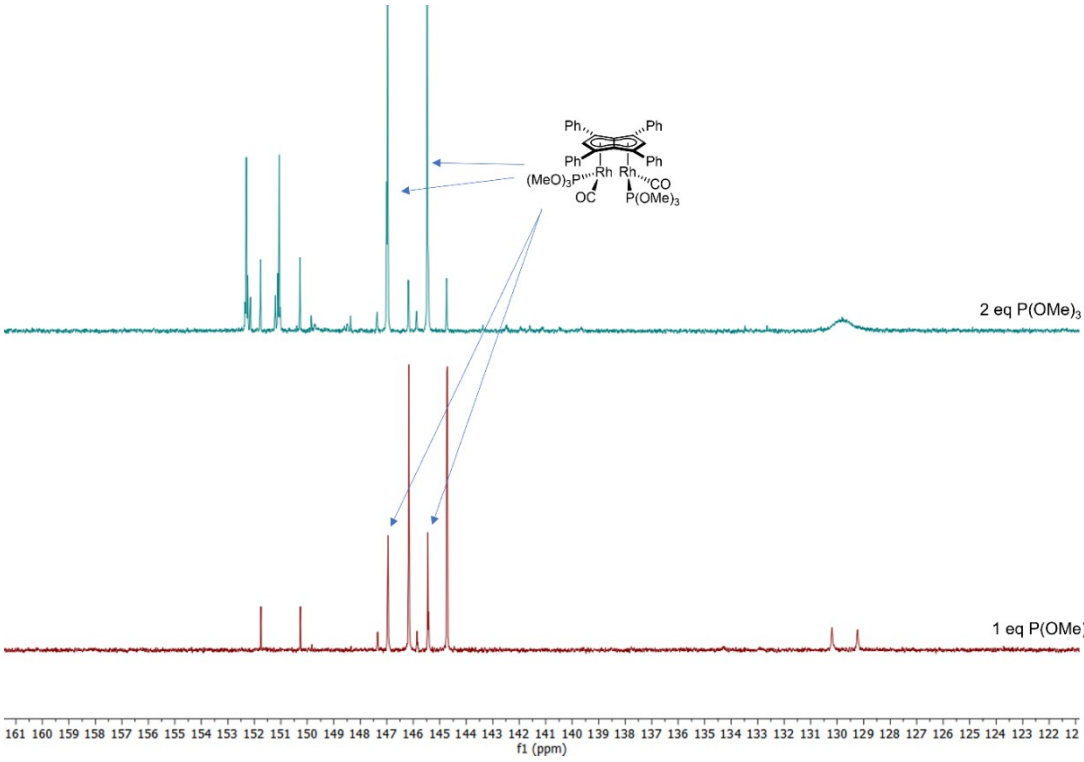

Figure S55: 202 MHz $^{31}P\{^{1}H\}$ NMR spectra of addition of $P(OMe)_3$ to $[Rh^{I}(CO)_2]_2[\mu:\eta^5:\eta^5Ph_4Pn]$ in THF-H_8

UV-vis Spectra of **5**, **6** and **11**

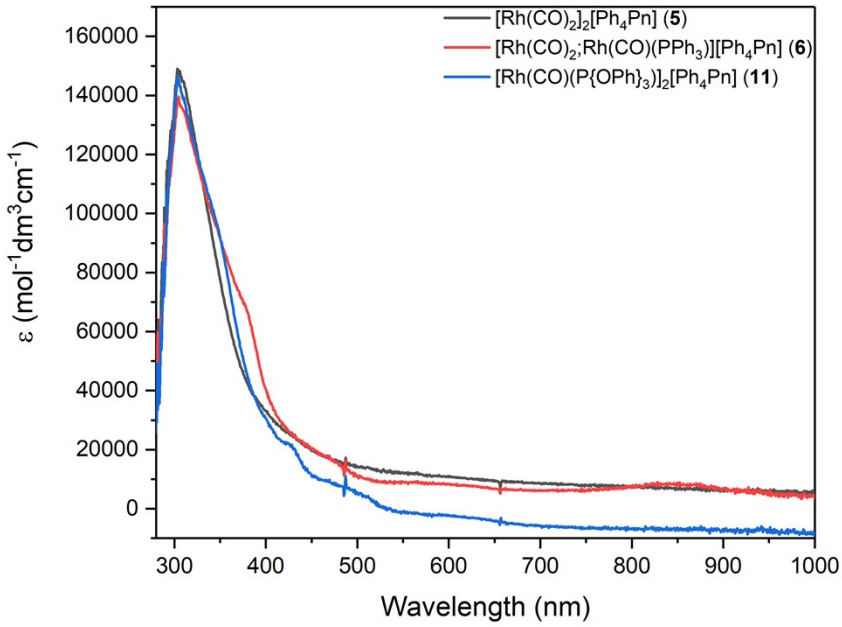

Figure S56: UV-vis spectra of $[Rh^{I}(CO)_2]_2[Ph_4Pn]$, $[Rh^{I}(CO)_2;Rh^{I}(CO)(PPh_3)][Ph_4Pn]$ and $[Rh^{I}(CO)(P\{OPh\}_3)]_2[Ph_4Pn]$ recorded at 1.5 x 10^{-6} M in THF at 298K

Near-IR Spectra of **5**, **10** and **11**

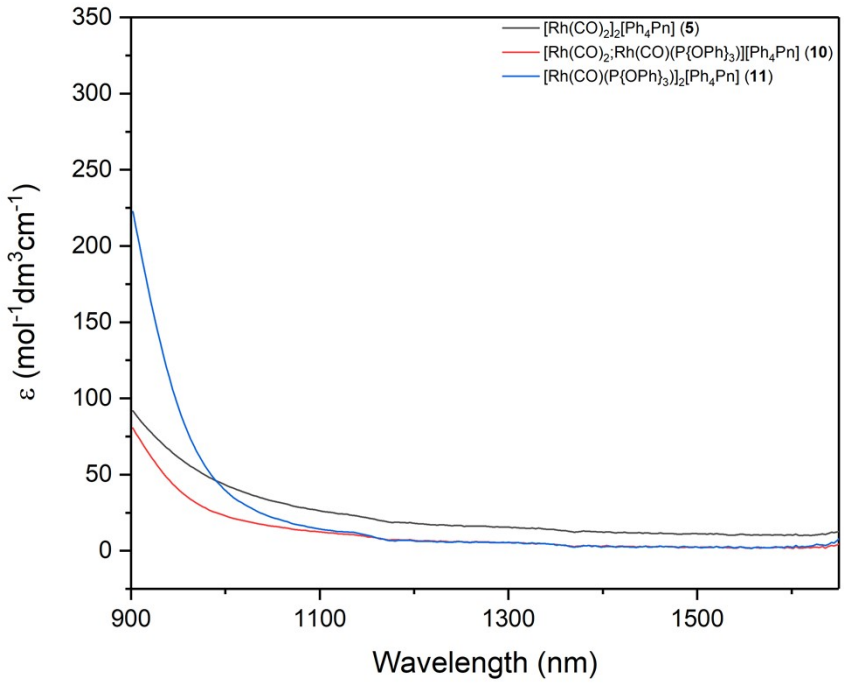

Figure S57: NIR spectra of $[Rh^{I}(CO)_2]_2[Ph_4Pn]$, $[Rh^{I}(CO)_2;Rh^{I}(CO)(P\{OPh\}_3)][Ph_4Pn]$ and $[Rh^{I}(CO)(P\{OPh\}_3)]_2[Ph_4Pn]$ recorded at 1.5 x 10^{-5} M in THF at 298K

Computational Data

Methodology

DFT calculations were run with Gaussian 16 (C.01).[1] The Rh centres were described with the Stuttgart RECPs and associated basis sets,[2] and the 6-31G** basis sets were used for all other atoms (BS1).[3,4] Initial BP86[5,6] optimizations were performed using the 'grid = ultrafine' option, with all stationary points being fully characterized via analytical frequency calculations as minima (all positive eigenvalues). All energies were recomputed with a larger basis set featuring 6-311++G** on all atoms, with the exception of Rh (aug-cc-pVTZ-PP). Natural Bonding Orbital (NBO7)[7] analyses were performed on the BP86/BS1-optmised geometries with a larger basis set featuring 6-311++G** on all atoms, with the exception of Rh (aug-cc-pVTZ-PP) within Gaussian 16 (C.01).

Breakdown of Energy Contributions

The following tables detail the evolution of the relative energies as the successive corrections to the initial SCF energy are included. Terms used are:

ΔE_{BSI}	SCF energy computed with the BP86 functional with BS1
ΔH_{BSI}	Enthalpy at 0 K with BS1
ΔG_{BSI}	Free energy at 298.15 K and 1 atm with BS1
$\Delta G_{BSI/THF}$	Free energy corrected for THF solvent with BS1
$\Delta G_{BSI/THF+D3BJ}$	Free energy corrected for THF and dispersion effects with BS1
ΔE_{BS2}	SCF energy computed with the BP86 functional with BS2
ΔG_{THF}	Free energy corrected for basis set (BS2), dispersion effects and THF solvent

In each case the final data used in the main article are highlighted in bold

Table S1. Relative energies for computed structures. Data in bold are those used in the main text. Free energies are quoted relative to synthesised complexes, **4** and **5,** at 0.0 kcal mol^{-1}.

	ΔE_{BSI}	ΔH_{BSI}	ΔG_{BSI}	$\Delta G_{BSI/THF}$	$\Delta G_{BSI/THF+D3BJ}$	ΔE_{BS2}	ΔG_{THF}
4	0.0	0.0	0.0	0.0	0.0	0.0	**0.0**
4-syn	1.9	2.6	3.6	3.8	0.6	2.4	**1.2**
5	0.0	0.0	0.0	0.0	0.0	0.0	**0.0**
5-anti	1.6	1.5	1.4	2.3	5.0	1.2	**4.6**

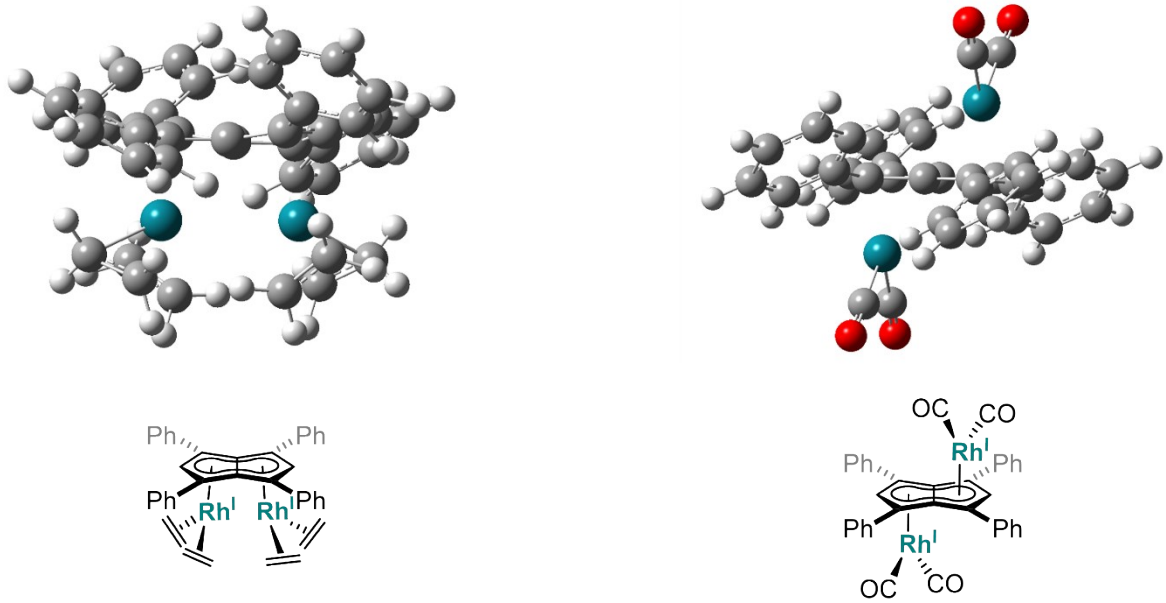

Figure S58 – DFT optimised geometries of theoretical species, ***syn*-[Rh(C_2H_4)$_2$]$_2$[Ph_4Pn]** (***syn-4,*** left) and ***anti*-[Rh(CO)$_2$]$_2$[Ph_4Pn]** (***anti*-5**, right) using BP86-D3BJ(THF)/BS2//BP86/BS1

NBO Data

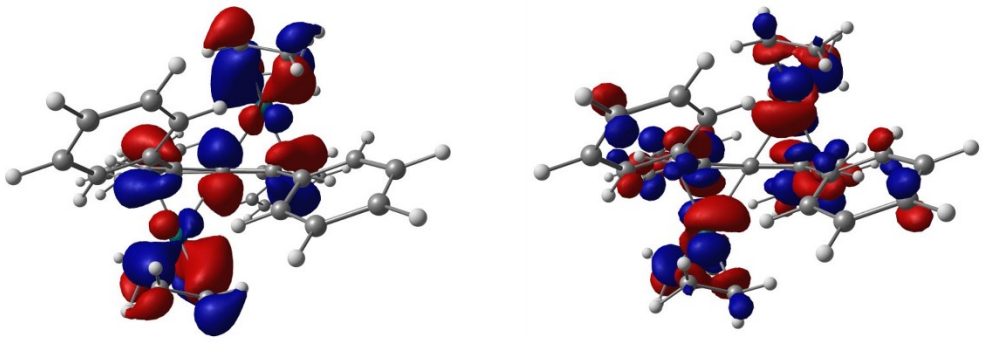

HOMO (−4.73 eV) LUMO (−2.29 eV)

Figure S59 - HOMO (left) and LUMO (right) of ***anti*-[Rh(C_2H_4)$_2$]$_2$[Ph_4Pn]** (**4**)

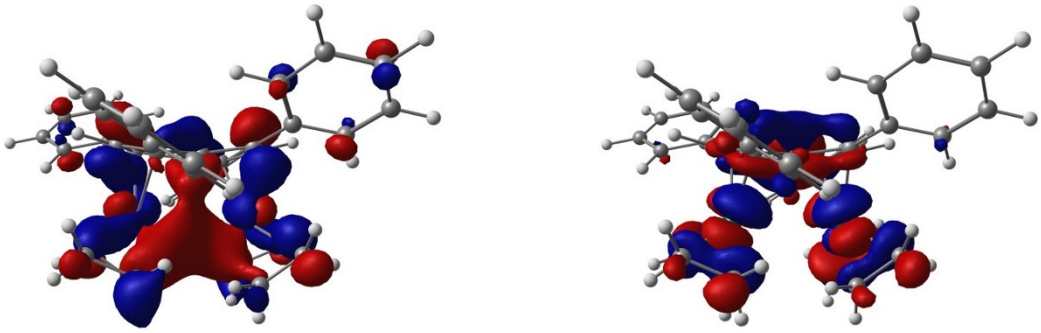

HOMO (−4.63 eV) LUMO (−2.48 eV)

Figure S60 - HOMO (left) and LUMO (right) of ***syn*-[Rh(C_2H_4)$_2$]$_2$[Ph_4Pn]** (***syn-4***)

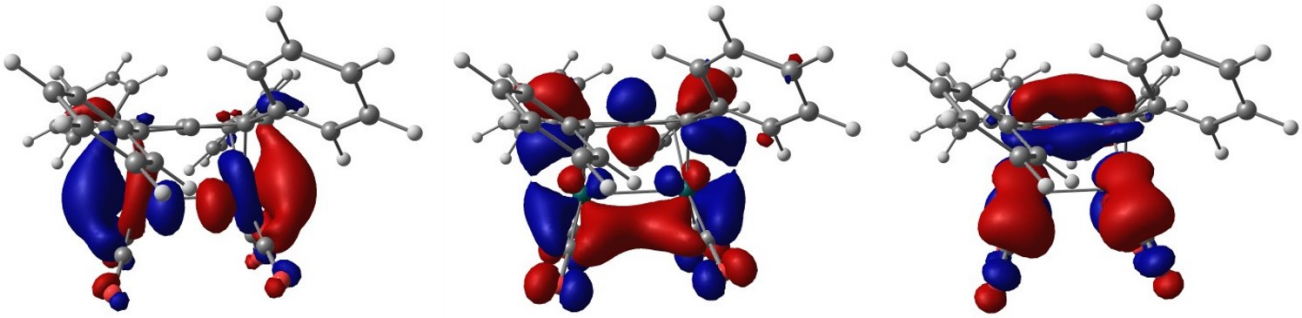

HOMO−1 (−5.39 eV) HOMO (−5.20 eV) LUMO (−3.24 eV)

Figure S61 - HOMO−1, HOMO and LUMO of ***syn*-[Rh(CO)$_2$]$_2$[Ph_4Pn]** (**5**)

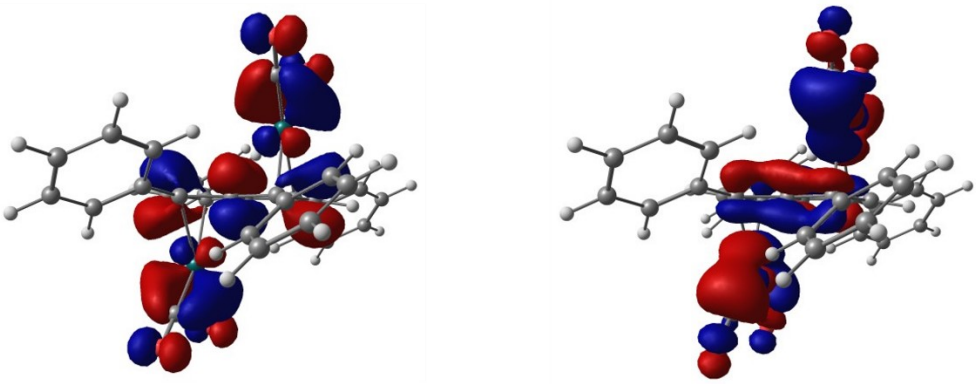

HOMO (−5,12 eV) LUMO (−2.99 eV)

Figure S62 - HOMO (left) and LUMO (right) of ***anti*-[Rh(CO)$_2$]$_2$[Ph_4Pn]** (***anti*-5**)

Table S2. Wiberg Bond Indices (WBI) data for the DFT-optimised structures **4-syn** and **5**

	***syn*-[Rh(C_2H_4)$_2$]$_2$[Ph_4Pn]**	***syn*-[Rh(CO)$_2$]$_2$[Ph_4Pn]**
Rh – Rh	0.0587	0.0448

Cartesian Coordinates and Computed Energies (in Hartrees) for Calculated Structures

***anti*-[Rh(C_2H_4)$_2$]$_2$[Ph_4Pn] (4)**

SCF (BP86) Energy = -1768.49137296
Enthalpy 0K = -1767.856404
Enthalpy 298K = -1767.814975
Free Energy 298K = -1767.929667
Lowest Frequency = 16.0002 cm^{-1}
Second Frequency = 19.9555 cm^{-1}
SCF (BP86-D3BJ) Energy = -1768.72819232
SCF (THF) Energy = -1768.49977223
SCF (BS2) Energy = -1768.19693388

Rh	-0.02738	2.02782	1.17761
C	0.72103	0.00006	-0.00001
C	1.19217	1.23215	-0.64452
C	2.55211	1.60245	-1.09854
C	3.49593	0.62132	-1.47940
H	3.24207	-0.43731	-1.38046
C	4.74715	0.99031	-1.99652
H	5.45992	0.21158	-2.28739
C	5.08290	2.34489	-2.14442
H	6.06035	2.63100	-2.54628
C	4.15522	3.33149	-1.76792
H	4.40844	4.39208	-1.87116
C	2.90667	2.96541	-1.24894
H	2.19289	3.73616	-0.93843
C	0.01744	1.94321	-1.06640
H	0.02909	2.81155	-1.72557
C	-1.18490	1.26770	-0.62260
C	-2.52620	1.70315	-1.08240
C	-2.78243	3.07686	-1.31929
H	-2.00078	3.81154	-1.10148
C	-4.01483	3.50807	-1.82589
H	-4.18551	4.57679	-1.99404
C	-5.02788	2.57756	-2.11313
H	-5.99244	2.91394	-2.50700
C	-4.78781	1.21295	-1.89295
H	-5.56256	0.47339	-2.12111
C	-3.55224	0.78079	-1.38729
H	-3.37483	-0.28566	-1.23659
C	-1.20134	3.66218	1.86058
H	-0.61989	4.35403	2.48368
H	-1.72986	4.14548	1.03098
C	-1.71286	2.45661	2.42684
H	-2.61769	2.01223	1.99727
H	-1.54755	2.21356	3.48202
C	1.68764	2.97305	2.06856
H	2.57123	2.74308	1.46055
H	1.53277	4.04394	2.24509
C	1.15412	2.00879	2.96727
H	0.59012	2.34023	3.84763
H	1.62676	1.02491	3.07761
C	-0.74289	0.00003	0.00000
C	-1.18486	-1.26768	0.62257
C	-2.52613	-1.70319	1.08238
C	-3.55217	-0.78087	1.38740
H	-3.37478	0.28560	1.23681
C	-4.78771	-1.21310	1.89308
H	-5.56247	-0.47358	2.12134
C	-5.02774	-2.57774	2.11315
H	-5.99227	-2.91418	2.50704
C	-4.01468	-3.50820	1.82579
H	-4.18533	-4.57694	1.99385
C	-2.78232	-3.07692	1.31917
H	-2.00066	-3.81157	1.10126
C	0.01751	-1.94314	1.06636
H	0.02919	-2.81145	1.72557
C	1.19222	-1.23205	0.64446
C	2.55215	-1.60230	1.09853
C	2.90675	-2.96524	1.24897
H	2.19300	-3.73602	0.93845
C	4.15529	-3.33129	1.76800
H	4.40853	-4.39186	1.87126
C	5.08294	-2.34465	2.14450
H	6.06038	-2.63073	2.54640
C	4.74715	-0.99008	1.99657
H	5.45989	-0.21133	2.28744
C	3.49593	-0.62114	1.47941
H	3.24205	0.43748	1.38045
Rh	-0.02723	-2.02789	-1.17762
C	1.68779	-2.97331	-2.06837
H	1.53280	-4.04418	-2.24485
H	2.57136	-2.74340	-1.46031
C	1.15444	-2.00904	-2.96718
H	1.62717	-1.02521	-3.07751
H	0.59047	-2.34048	-3.84756
C	-1.20130	-3.66212	-1.86074
H	-1.72999	-4.14537	-1.03122
H	-0.61983	-4.35402	-2.48376
C	-1.71261	-2.45650	-2.42706
H	-1.54715	-2.21346	-3.48222
H	-2.61742	-2.01199	-1.99759

***syn*-[Rh(C_2H_4)$_2$]$_2$[Ph_4Pn] (*syn*-4)**

SCF (BP86) Energy = -1768.48842457
Enthalpy 0K = -1767.852336
Enthalpy 298K = -1767.811293
Free Energy 298K = -1767.923952
Lowest Frequency = 22.5270 cm^{-1}
Second Frequency = 36.2811 cm^{-1}
SCF (BP86-D3BJ) Energy = -1768.73032093
SCF (THF) Energy = -1768.49648406
SCF (BS2) Energy = -1768.19309736

C	-1.18573	1.38197	-0.90876
C	0.00272	2.20103	-0.94563
H	0.00579	3.25829	-1.21172
C	1.18478	1.38977	-0.69057
C	0.72900	-0.00708	-0.70860
C	1.18580	-1.38138	-0.90894
C	-0.00256	-2.20047	-0.94620
H	-0.00551	-3.25766	-1.21256
C	-1.18472	-1.38937	-0.69099
C	-0.72903	0.00758	-0.70872
C	-2.50190	1.88850	-1.36794
C	-3.33575	1.10691	-2.20099
H	-3.03656	0.08835	-2.46005
C	-4.52753	1.63203	-2.72250
H	-5.15415	1.00552	-3.36598
C	-4.91091	2.95059	-2.43282
H	-5.84246	3.35779	-2.83946
C	-4.08440	3.74569	-1.62106
H	-4.36828	4.77832	-1.39117
C	-2.89625	3.22159	-1.09490
H	-2.25876	3.84486	-0.45914

C	2.57425	1.89928	-0.71073
C	2.89619	3.10896	-1.37276
H	2.11491	3.65395	-1.91212
C	4.20683	3.60783	-1.36885
H	4.42958	4.54328	-1.89312
C	5.22989	2.90997	-0.70624
H	6.25307	3.29943	-0.70457
C	4.92879	1.70522	-0.05018
H	5.71734	1.14778	0.46603
C	3.61870	1.20630	-0.05109
H	3.39488	0.26387	0.45824
C	2.50204	-1.88763	-1.36824
C	3.33562	-1.10588	-2.20140
H	3.03620	-0.08736	-2.46039
C	4.52741	-1.63079	-2.72309
H	5.15383	-1.00419	-3.36667
C	4.91109	-2.94927	-2.43342
H	5.84265	-3.35629	-2.84019
C	4.08488	-3.74451	-1.62148
H	4.36904	-4.77705	-1.39156
C	2.89671	-3.22062	-1.09516
H	2.25946	-3.84393	-0.45919
C	-2.57406	-1.89921	-0.71136
C	-2.89559	-3.10909	-1.37324
H	-2.11412	-3.65399	-1.91240
C	-4.20609	-3.60831	-1.36946
H	-4.42848	-4.54391	-1.89362
C	-5.22947	-2.91062	-0.70718
H	-6.25255	-3.30035	-0.70561
C	-4.92880	-1.70568	-0.05128
H	-5.71759	-1.14833	0.46469
C	-3.61883	-1.20641	-0.05203
H	-3.39540	-0.26383	0.45717
Rh	-0.11851	1.63127	1.15747
Rh	0.11825	-1.63148	1.15716
C	1.00900	3.21111	2.01399
C	1.45335	1.97417	2.57220
H	0.39553	3.89507	2.61401
H	1.60851	3.70639	1.24020
H	1.20118	1.70488	3.60356
H	2.38711	1.53572	2.19901
C	-1.44619	1.42406	2.86096
C	-1.87448	2.50685	2.05064
H	-0.92659	1.61719	3.80643
H	-1.96669	0.46521	2.81776
H	-1.69564	3.54412	2.35736
H	-2.72246	2.37922	1.36800
C	1.44417	-1.42660	2.86237
C	1.87528	-2.50610	2.04919
H	0.92400	-1.62374	3.80671
H	1.96291	-0.46666	2.82269
H	1.69826	-3.54468	2.35253
H	2.72351	-2.37466	1.36760
C	-1.00778	-3.21227	2.01361
C	-1.45453	-1.97565	2.57063
H	-0.39383	-3.89494	2.61463
H	-1.60588	-3.70897	1.23964
H	-1.20389	-1.70526	3.60208
H	-2.38847	-1.53874	2.19607

***syn*-[Rh(CO)$_2$]$_2$[Ph$_4$Pn] (5)**

SCF (BP86) Energy = -1907.48671547
Enthalpy 0K = -1907.031402
Enthalpy 298K = -1906.991886
Free Energy 298K = -1907.106987
Lowest Frequency = 19.7728 cm^{-1}
Second Frequency = 30.1757 cm^{-1}
SCF (BP86-D3BJ) Energy = -1907.68722449
SCF (THF) Energy = -1907.49678106
SCF (BS2) Energy = -1907.26206118

C	1.21833	-1.36836	-0.91296
C	0.04646	-2.21756	-0.99351
H	0.07125	-3.28875	-1.19118
C	-1.15200	-1.41976	-0.80739
C	-0.72339	-0.01214	-0.86008
C	-1.21833	1.36858	-0.91299
C	-0.04651	2.21779	-0.99331
H	-0.07126	3.28901	-1.19083
C	1.15197	1.41995	-0.80722
C	0.72342	0.01238	-0.86012
C	2.59068	-1.85390	-1.21535
C	3.39847	-1.17510	-2.15411
H	3.03432	-0.25138	-2.61325
C	4.65670	-1.68294	-2.51173
H	5.26908	-1.14149	-3.24015
C	5.12685	-2.87652	-1.94278
H	6.11043	-3.26940	-2.22028
C	4.32810	-3.56339	-1.01267
H	4.68748	-4.49306	-0.55916
C	3.07217	-3.05735	-0.65205
H	2.45598	-3.58258	0.08585
C	-2.53660	-1.95313	-0.87796
C	-2.82927	-3.05334	-1.71510
H	-2.03477	-3.49131	-2.32835
C	-4.12935	-3.57673	-1.78194
H	-4.33614	-4.42934	-2.43720
C	-5.15958	-3.00802	-1.01685
H	-6.17366	-3.41757	-1.06699
C	-4.88143	-1.90912	-0.18615
H	-5.67705	-1.45934	0.41640
C	-3.58400	-1.38505	-0.11795
H	-3.37207	-0.53861	0.54235
C	-2.59071	1.85414	-1.21521
C	-3.39827	1.17580	-2.15451
H	-3.03392	0.25240	-2.61415
C	-4.65653	1.68368	-2.51198
H	-5.26874	1.14260	-3.24082
C	-5.12693	2.87684	-1.94234
H	-6.11054	3.26975	-2.21973
C	-4.32841	3.56324	-1.01168
H	-4.68800	4.49257	-0.55764
C	-3.07246	3.05715	-0.65121
H	-2.45642	3.58201	0.08710
C	2.53656	1.95341	-0.87766
C	2.82926	3.05353	-1.71489
H	2.03481	3.49140	-2.32827
C	4.12934	3.57698	-1.78164
H	4.33616	4.42952	-2.43697
C	5.15950	3.00840	-1.01638
H	6.17357	3.41799	-1.06643
C	4.88131	1.90957	-0.18558

H	5.67689	1.45990	0.41710
C	3.58390	1.38545	-0.11747
H	3.37192	0.53905	0.54288
C	-1.11907	-1.98827	2.38709
C	1.54570	-1.69182	2.29961
C	-1.54547	1.69015	2.30020
C	1.11902	1.98881	2.38694
O	-1.88807	-2.34822	3.19116
O	2.43172	-1.85028	3.04708
O	-2.43137	1.84761	3.04802
O	1.88793	2.34907	3.19096
Rh	0.13322	-1.48427	1.09147
Rh	-0.13317	1.48407	1.09155

***anti*-[Rh(CO)$_2$]$_2$[Ph$_4$Pn] (*anti*-5)**

SCF (BP86) Energy = -1907.48422317
Enthalpy 0K = -1907.029008
Enthalpy 298K = -1906.989346
Free Energy 298K = -1907.104728
Lowest Frequency = 24.9880 cm^{-1}
Second Frequency = 31.5320 cm^{-1}
SCF (BP86-D3BJ) Energy = -1907.68055560
SCF (THF) Energy = -1907.49283916
SCF (BS2) Energy = -1907.26007984

Rh	0.00045	-2.18984	-0.89983
C	0.72477	-0.00041	-0.00018
C	1.18618	-1.16214	0.78020
C	2.55473	-1.48089	1.25693
C	3.45884	-0.44893	1.59031
H	3.16637	0.59453	1.44441
C	4.72044	-0.75293	2.12447
H	5.40742	0.06059	2.37908
C	5.09875	-2.08811	2.33210
H	6.08530	-2.32345	2.74442
C	4.20544	-3.12264	2.00332
H	4.49503	-4.16790	2.15363
C	2.94509	-2.82261	1.47123
H	2.25638	-3.62893	1.19541
C	0.00029	-1.78748	1.31649
H	0.00042	-2.58179	2.06277
C	-1.18573	-1.16247	0.78026
C	-2.55419	-1.48162	1.25702
C	-2.94447	-2.82350	1.47047
H	-2.25577	-3.62959	1.19395
C	-4.20472	-3.12393	2.00263
H	-4.49425	-4.16930	2.15226
C	-5.09796	-2.08963	2.33230
H	-6.08443	-2.32525	2.74466
C	-4.71973	-0.75429	2.12550
H	-5.40668	0.05902	2.38082
C	-3.45825	-0.44990	1.59129
H	-3.16581	0.59366	1.44602
C	-0.72468	-0.00069	-0.00022
C	-1.18612	1.16182	-0.77963
C	-2.55464	1.48042	-1.25654
C	-3.45894	0.44850	-1.58948
H	-3.16665	-0.59495	-1.44321
C	-4.72051	0.75248	-2.12375
H	-5.40760	-0.06105	-2.37801
C	-5.09863	2.08761	-2.33194
H	-6.08515	2.32292	-2.74434
C	-4.20514	3.12215	-2.00360
H	-4.49455	4.16739	-2.15434
C	-2.94485	2.82212	-1.47139
H	-2.25603	3.62846	-1.19588
C	-0.00021	1.78713	-1.31603
H	-0.00028	2.58134	-2.06241
C	1.18584	1.16220	-0.77975
C	2.55425	1.48124	-1.25673
C	2.94448	2.82310	-1.47044
H	2.25578	3.62921	-1.19396
C	4.20465	3.12350	-2.00277
H	4.49412	4.16885	-2.15262
C	5.09793	2.08919	-2.33233
H	6.08435	2.32480	-2.74482
C	4.71978	0.75389	-2.12526
H	5.40673	-0.05946	-2.38047
C	3.45835	0.44953	-1.59089
H	3.16596	-0.59403	-1.44547
Rh	-0.00043	2.19065	0.89950
C	-1.34180	3.01268	1.90339
C	1.34040	3.01173	1.90496
O	2.16944	3.55896	2.52362
O	-2.17127	3.56058	2.52090
C	-1.34038	-3.01093	-1.90519
C	1.34145	-3.01230	-1.90378
O	-2.16947	-3.55817	-2.52379
O	2.17058	-3.56067	-2.52134

References

(1) Frisch, M. J.; Trucks, G. W.; Schlegel, H. B.; Scuseria, G. E.; Robb, M. A.; Cheeseman, J. R. Scalmani, G.; Barone, V.; Petersson, G. A.; Nakatsuji, H.; Li, X.; Caricato, M.; Marenich, A. V.; Bloino, J.; Janesko, B. G.; Gomperts, R.; Mennucci, B.; Hratchian, H. P.; Ortiz, J. V.; Izmaylov, A. F.; Sonnenberg, J. L.; Williams-Young, D.; Ding, F.; Lipparini, F.; Egidi, F.; Goings, J.; Peng, B.; Petrone, A.; Henderson, T.; Ranasinghe, D.; Zakrzewski, V. G.; Gao, J.; Rega, N.; Zheng, G.; Liang, W.; Hada, M.; Ehara, M.; Toyota, K.; Fukuda, R.; Hasegawa, J.; Ishida, M.; Nakajima, T.; Honda, Y.; Kitao, O.; Nakai, H.; Vreven, T.; Throssell, K.; Montgomery, J. A., J.; Peralta, J. E.; Ogliaro, F.; Bearpark, M. J.; Heyd, J. J.; Brothers, E. N.; Kudin, K. N.; Staroverov, V. N.; Keith, T. A.; Kobayashi, R.; Normand, J.; Raghavachari, K.; Rendell, A. P.; Burant, J. C.; Iyengar, S. S.; Tomasi, J.; Cossi, M.; Millam, J. M.; Klene, M.; Adamo, C.; Cammi, R.; Ochterski, J. W.; Martin, R. L.; Morokuma, K.; Farkas, O.; Foresman, J. B.; Fox, D. J. Gaussian 16, Revision C.01., Gaussian Inc., Wallingford CT 2016.

(2) Andrae, D.; Häußermann, U.; Dolg, M.; Stoll, H.; Preuß, H. Energy-Adjusted Ab Initio Pseudopotentials for the Second and Third Row Transition Elements. *Theor. Chim. Acta* **1990**, *77* (2), 123–141. https://doi.org/10.1007/BF01114537

(3) Hariharan, P. C.; Pople, J. A. The Influence of Polarization Functions on Molecular Orbital Hydrogenation Energies. *Theor. Chim. Acta* **1973**, *28* (3), 213–222. https://doi.org/10.1007/BF00533485.

(4) Hehre, W. J.; Ditchfield, R.; Pople, J. A.; Wall, F. T.; Hiller, L. A.; Wheeler, D. J.; Chern Phys, J.; Hammersley, J. M.; Morton, K. W.; Roy Stat Soc, J.; Herre, W. J.; Ditcrfield, R. Self—Consistent Molecular Orbital Methods. XII. Further Extensions of Gaussian—Type Basis Sets for Use in Molecular Orbital Studies of Organic Molecules. *J. Chem. Phys.* **1972**, *56* (5), 2257–2261. https://doi.org/10.1063/1.1677527.

(5) Becke, A. D. Density-Functional Exchange-Energy Approximation with Correct Asymptotic Behavior. *Phys. Rev. A* **1988**, *38* (6), 3098. https://doi.org/10.1103/PhysRevA.38.3098.

(6) Perdew, J. P. Density-Functional Approximation for the Correlation Energy of the Inhomogeneous Electron Gas. *Phys. Rev. B* **1986**, *33* (12), 8822. https://doi.org/10.1103/PhysRevB.33.8822.

(7) Glendening, E. D.; Badenhoop, J. K.; Reed, A. E.; Carpenter, J. E.; Bohmann, J. A.; Morales, C. M.; Karafiloglou, P.; Landis, C. R.; Weinhold, F., NBO 7.0. Theoretical Chemistry Institute, University of Wisconsin: Madison 2018.

Crystallographic Data

Anti-[Rh^{I}(COD)]$_2$[μ:η^5:$\eta^5$$Ph_4$Pn] (**1**)

CCDC	**2309145**	
Identification code	s21uh9	
Empirical formula	C_{48} H_{46} Rh_2	
Formula weight	828.67	
Temperature	150.00(10) K	
Wavelength	0.71073 Å	
Crystal system	Monoclinic	
Space group	$P2_1/n$	
Unit cell dimensions	a = 11.0316(2) Å	α = 90°
	b = 20.0004(3) Å	β = 96.9761(19)°
	c = 16.3232(3) Å	γ = 90°
Volume	3574.83(11) $Å^3$	
Z	4	
Density (calculated)	1.540 Mg/m^3	
Absorption coefficient	0.958 mm^{-1}	
F(000)	1696	
Crystal size	0.430 x 0.302 x 0.179 mm^3	
Theta range for data collection	3.236 to 27.485°	
Index ranges	-14<=h<=14, -25<=k<=25, -21<=l<=20	
Reflections collected	32896	
Independent reflections	8194 [R(int) = 0.0275]	
Completeness to theta = 25.242°	99.8 %	
Absorption correction	Semi-empirical from equivalents	
Max. and min. transmission	1.00000 and 0.82879	
Refinement method	Full-matrix least-squares on F^2	
Data / restraints / parameters	8194 / 0 / 451	
Goodness-of-fit on F^2	1.055	
Final R indices [I>2sigma(I)]	R1 = 0.0308, wR2 = 0.0768	
R indices (all data)	R1 = 0.0363, wR2 = 0.0801	
Extinction coefficient	n/a	
Largest diff. peak and hole	2.385 and -0.392 e.$Å^{-3}$	

Anti-[Ir^{I}(COD)]$_2$[μ:η^5:η^5Ph$_4$Pn] (**2**)

CCDC	**2309146**	
Identification code	s21uh8	
Empirical formula	$C_{48}H_{46}Ir_2$	
Formula weight	1007.25	
Temperature	150.00(10) K	
Wavelength	0.71073 Å	
Crystal system	Monoclinic	
Space group	$P2_1/n$	
Unit cell dimensions	a = 10.4071(2) Å	α = 90°
	b = 18.5544(5) Å	β = 103.209(2)°
	c = 19.0926(4) Å	γ = 90°
Volume	3589.19(14) Å^3	
Z	4	
Density (calculated)	1.864 Mg/m^3	
Absorption coefficient	7.442 mm^{-1}	
F(000)	1952	
Crystal size	0.606 x 0.211 x 0.087 mm^3	
Theta range for data collection	3.328 to 27.482°	
Index ranges	-13<=h<=13, -24<=k<=22, -24<=l<=24	
Reflections collected	39304	
Independent reflections	8218 [R(int) = 0.0504]	
Completeness to theta = 25.242°	99.8 %	
Absorption correction	Semi-empirical from equivalents	
Max. and min. transmission	1.00000 and 0.35394	
Refinement method	Full-matrix least-squares on F^2	
Data / restraints / parameters	8218 / 0 / 451	
Goodness-of-fit on F^2	1.075	
Final R indices [I>2sigma(I)]	R1 = 0.0320, wR2 = 0.0636	
R indices (all data)	R1 = 0.0414, wR2 = 0.0676	
Extinction coefficient	n/a	
Largest diff. peak and hole	1.484 and -2.054 e.Å^{-3}	

Anti-[Rh^{I}(NBD)]$_2$[μ:η^5:η^5Ph$_4$Pn] (**3**)

CCDC	**2309147**	
Identification code	s22uh33	
Empirical formula	C_{54} H_{54} O_2 Rh_2	
Formula weight	940.79	
Temperature	150.00(10) K	
Wavelength	1.54184 Å	
Crystal system	Monoclinic	
Space group	I2/a	
Unit cell dimensions	a = 10.72484(18) Å	α = 90°
	b = 15.12621(19) Å	β = 96.9831(15)°
	c = 26.3385(4) Å	γ = 90°
Volume	4241.10(11) Å^3	
Z	4	
Density (calculated)	1.473 Mg/m^3	
Absorption coefficient	6.611 mm^{-1}	
F(000)	1936	
Crystal size	0.132 x 0.099 x 0.042 mm^3	
Theta range for data collection	5.080 to 68.248°	
Index ranges	-12<=h<=10, -18<=k<=18, -31<=l<=31	
Reflections collected	47478	
Independent reflections	3876 [R(int) = 0.0478]	
Completeness to theta = 67.684°	99.9 %	
Absorption correction	Semi-empirical from equivalents	
Max. and min. transmission	1.00000 and 0.68951	
Refinement method	Full-matrix least-squares on F^2	
Data / restraints / parameters	3876 / 72 / 307	
Goodness-of-fit on F^2	1.147	
Final R indices [I>2sigma(I)]	R1 = 0.0893, wR2 = 0.2285	
R indices (all data)	R1 = 0.0897, wR2 = 0.2288	
Extinction coefficient	n/a	
Largest diff. peak and hole	5.393 and -1.756 e.Å^{-3}	

Anti-[$Rh^{I}(C_2H_4)_2]_2[\mu:\eta^5:\eta^5Ph_4Pn]$ (**4**)

CCDC	**2309148**	
Identification code	s23uh11	
Empirical formula	$C_{48}\ H_{54}\ O_4\ Rh_2$	
Formula weight	900.73	
Temperature	150.01(10) K	
Wavelength	1.54184 Å	
Crystal system	Triclinic	
Space group	P-1	
Unit cell dimensions	a = 11.45331(12) Å	α = 70.0281(12)°
	b = 11.67087(14) Å	β = 85.1666(10)°
	c = 16.3454(2) Å	γ = 76.5215(10)°
Volume	1996.91(4) $Å^3$	
Z	2	
Density (calculated)	1.498 Mg/m^3	
Absorption coefficient	7.028 mm^{-1}	
F(000)	928	
Crystal size	0.200 x 0.180 x 0.120 mm^3	
Theta range for data collection	3.969 to 72.932°	
Index ranges	-14<=h<=13, -14<=k<=14, -20<=l<=20	
Reflections collected	44268	
Independent reflections	7923 [R(int) = 0.0221]	
Completeness to theta = 67.684°	99.9 %	
Absorption correction	Semi-empirical from equivalents	
Max. and min. transmission	1.00000 and 0.62331	
Refinement method	Full-matrix least-squares on F^2	
Data / restraints / parameters	7923 / 0 / 487	
Goodness-of-fit on F^2	1.071	
Final R indices [I>2sigma(I)]	R1 = 0.0218, wR2 = 0.0573	
R indices (all data)	R1 = 0.0222, wR2 = 0.0575	
Extinction coefficient	n/a	
Largest diff. peak and hole	0.550 and -0.589 e.$Å^{-3}$	

Syn-[Rh^{I}(CO)$_2$]$_2$[μ:η^5:η^5Ph$_4$Pn] (**5**)

CCDC	**2309149**	
Identification code	s22uh4	
Empirical formula	C_{36} H_{22} O_4 Rh_2	
Formula weight	724.35	
Temperature	150.01(10) K	
Wavelength	0.71073 Å	
Crystal system	Monoclinic	
Space group	$P2_1/n$	
Unit cell dimensions	a = 12.7037(2) Å	α = 90°
	b = 10.34448(16) Å	β = 103.7600(16)°
	c = 22.6879(4) Å	γ = 90°
Volume	2895.92(8) Å^3	
Z	4	
Density (calculated)	1.661 Mg/m^3	
Absorption coefficient	1.179 mm^{-1}	
F(000)	1440	
Crystal size	0.472 x 0.421 x 0.090 mm^3	
Theta range for data collection	3.302 to 27.497°	
Index ranges	-16<=h<=16, -13<=k<=13, -29<=l<=29	
Reflections collected	44989	
Independent reflections	6633 [R(int) = 0.0305]	
Completeness to theta = 25.242°	99.8 %	
Absorption correction	Gaussian	
Max. and min. transmission	1.000 and 0.264	
Refinement method	Full-matrix least-squares on F^2	
Data / restraints / parameters	6633 / 0 / 379	
Goodness-of-fit on F^2	1.111	
Final R indices [I>2sigma(I)]	R1 = 0.0231, wR2 = 0.0509	
R indices (all data)	R1 = 0.0266, wR2 = 0.0525	
Extinction coefficient	n/a	
Largest diff. peak and hole	0.436 and -0.299 e.Å^{-3}	

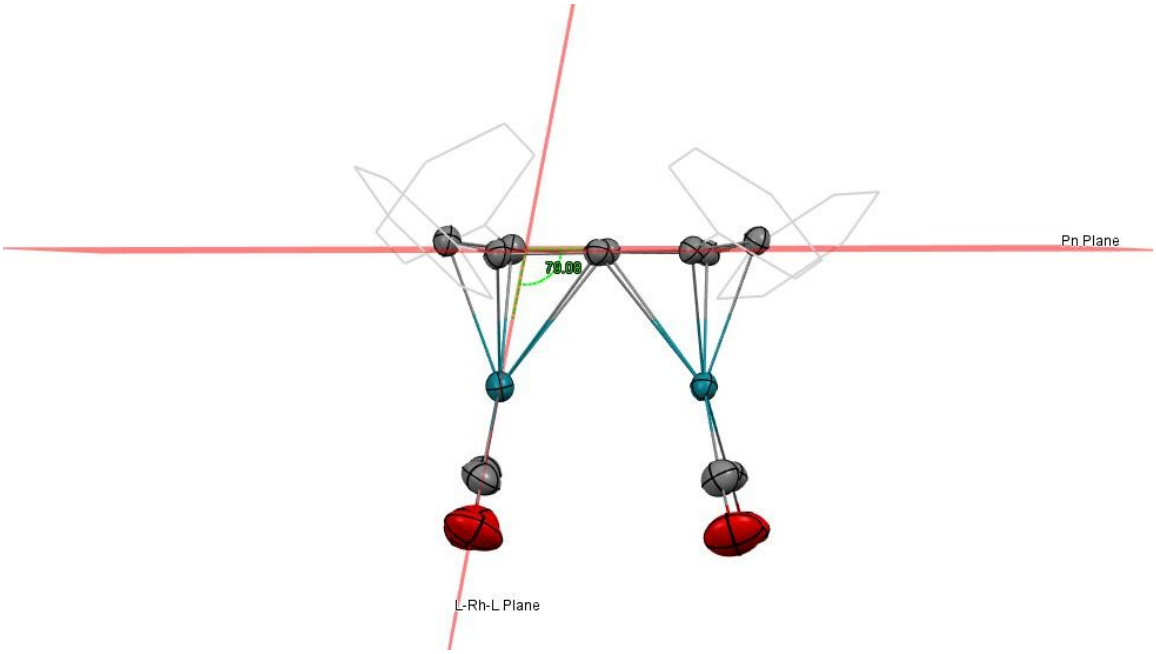

Figure S63: Definition of the dihedral between L-Rh-L plane and the plane of $\mathbf{Ph_4Pn^{2-}}$. Value given in main text is the average of each L-Rh-L plane (79.08° and 76.60°)

$[Rh^{II}(CO)(PMe_3)_4][Ph_4Pn]$ (**8**)

CCDC	**2309150**	
Identification code	s22uh24	
Empirical formula	$C_{102}\ H_{140}\ O_5\ P_8\ Rh_2$	
Formula weight	1899.71	
Temperature	150.00(10) K	
Wavelength	0.71073 Å	
Crystal system	Triclinic	
Space group	P-1	
Unit cell dimensions	a = 12.6981(2) Å	α = 76.340(2)°
	b = 13.2480(3) Å	β = 69.8125(19)°
	c = 17.4462(4) Å	γ = 63.790(2)°
Volume	2459.11(10) $Å^3$	
Z	1	
Density (calculated)	1.283 Mg/m^3	
Absorption coefficient	0.516 mm^{-1}	
F(000)	1002	
Crystal size	0.320 x 0.200 x 0.120 mm^3	
Theta range for data collection	3.374 to 30.550°	
Index ranges	-17<=h<=17, -18<=k<=18, -23<=l<=23	
Reflections collected	44004	
Independent reflections	13180 [R(int) = 0.0292]	
Completeness to theta = 25.242°	99.8 %	
Absorption correction	Semi-empirical from equivalents	
Max. and min. transmission	1.00000 and 0.97819	
Refinement method	Full-matrix least-squares on F^2	
Data / restraints / parameters	13180 / 15 / 608	
Goodness-of-fit on F^2	1.039	
Final R indices [I>2sigma(I)]	R1 = 0.0291, wR2 = 0.0673	
R indices (all data)	R1 = 0.0346, wR2 = 0.0699	
Extinction coefficient	n/a	
Largest diff. peak and hole	0.850 and -0.456 e.$Å^{-3}$	

$[Rh^{I}(dppe)_2][Rh^{I}(CO)_2(\eta^5\text{-}Ph_4Pn)]$ (**9**)

CCDC	**2309151**	
Identification code	s22uh32	
Empirical formula	$C_{102}\ H_{102}\ O_6\ P_4\ Rh_2$	
Formula weight	1753.53	
Temperature	150.00(10) K	
Wavelength	1.54184 Å	
Crystal system	Triclinic	
Space group	P-1	
Unit cell dimensions	a = 13.9687(3) Å	α = 75.3403(16)°
	b = 14.9315(3) Å	β = 87.2098(15)°
	c = 22.8545(4) Å	γ = 79.4900(15)°
Volume	4534.28(16) $Å^3$	
Z	2	
Density (calculated)	1.284 Mg/m^3	
Absorption coefficient	4.022 mm^{-1}	
F(000)	1824	
Crystal size	0.153 x 0.128 x 0.035 mm^3	
Theta range for data collection	3.784 to 72.980°	
Index ranges	-17<=h<=16, -18<=k<=17, -28<=l<=18	
Reflections collected	47619	
Independent reflections	17878 [R(int) = 0.0430]	
Completeness to theta = 67.684°	99.9 %	
Absorption correction	Semi-empirical from equivalents	
Max. and min. transmission	1.00000 and 0.82514	
Refinement method	Full-matrix least-squares on F^2	
Data / restraints / parameters	17878 / 10 / 1082	
Goodness-of-fit on F^2	1.115	
Final R indices [I>2sigma(I)]	R1 = 0.0555, wR2 = 0.1492	
R indices (all data)	R1 = 0.0636, wR2 = 0.1549	
Extinction coefficient	n/a	
Largest diff. peak and hole	1.496 and -1.079 e.$Å^{-3}$	

$[Mg_2(\mu\text{-}Cl)_3][Rh^I(CO)_2(\eta^5\text{-}Ph_4Pn)]$

CCDC	**2309152**	
Identification code	s22uh22	
Empirical formula	$C_{58}\ H_{70}\ Cl_3\ Mg_2\ O_8\ Rh$	
Formula weight	1153.02	
Temperature	150.00(10) K	
Wavelength	1.54184 Å	
Crystal system	Monoclinic	
Space group	$P2_1/c$	
Unit cell dimensions	a = 18.23888(15) Å	α = 90°
	b = 14.65593(8) Å	β = 103.8749(9)°
	c = 21.64988(19) Å	γ = 90°
Volume	5618.32(8) $Å^3$	
Z	4	
Density (calculated)	1.363 Mg/m^3	
Absorption coefficient	4.409 mm^{-1}	
F(000)	2408	
Crystal size	0.241 x 0.055 x 0.030 mm^3	
Theta range for data collection	3.677 to 72.955°	
Index ranges	-22<=h<=22, -18<=k<=11, -26<=l<=26	
Reflections collected	65504	
Independent reflections	11168 [R(int) = 0.0473]	
Completeness to theta = 67.684°	100.0 %	
Absorption correction	Semi-empirical from equivalents	
Max. and min. transmission	1.00000 and 0.76675	
Refinement method	Full-matrix least-squares on F^2	
Data / restraints / parameters	11168 / 36 / 677	
Goodness-of-fit on F^2	1.023	
Final R indices [I>2sigma(I)]	R1 = 0.0316, wR2 = 0.0756	
R indices (all data)	R1 = 0.0376, wR2 = 0.0787	
Extinction coefficient	n/a	
Largest diff. peak and hole	0.555 and -0.536 e.$Å^{-3}$	

$[Rh^{I}(CO)(P\{OPh\}_3)]_2[\mu:\eta^5:\eta^5Ph_4Pn]$ (**11**)

CCDC	**2309153**	
Identification code	s23uh3	
Empirical formula	$C_{152}\ H_{128}\ O_{19}\ P_4\ Rh_4$	
Formula weight	2794.06	
Temperature	150.01(10) K	
Wavelength	1.54184 Å	
Crystal system	Monoclinic	
Space group	$P2_1/c$	
Unit cell dimensions	a = 14.00549(11) Å	α = 90°
	b = 19.39104(14) Å	β = 106.3340(8)°
	c = 23.86254(18) Å	γ = 90°
Volume	6219.04(8) $Å^3$	
Z	2	
Density (calculated)	1.492 Mg/m^3	
Absorption coefficient	5.282 mm^{-1}	
F(000)	2864	
Crystal size	0.150 x 0.080 x 0.030 mm^3	
Theta range for data collection	3.861 to 73.007°	
Index ranges	-17<=h<=16, -23<=k<=23, -29<=l<=27	
Reflections collected	61512	
Independent reflections	12365 [R(int) = 0.0571]	
Completeness to theta = 67.684°	100.0 %	
Absorption correction	Semi-empirical from equivalents	
Max. and min. transmission	1.00000 and 0.87710	
Refinement method	Full-matrix least-squares on F^2	
Data / restraints / parameters	12365 / 216 / 961	
Goodness-of-fit on F^2	1.052	
Final R indices [I>2sigma(I)]	R1 = 0.0316, wR2 = 0.0746	
R indices (all data)	R1 = 0.0360, wR2 = 0.0773	
Extinction coefficient	n/a	
Largest diff. peak and hole	0.528 and -0.499 e.$Å^{-3}$	

$[Rh^{I}(CO)(P\{OMe\}_3)]_2[\mu:\eta^5:\eta^5Ph_4Pn]$ (**12**)

CCDC	**2309154**	
Identification code	s23uh12	
Empirical formula	$C_{40}H_{40}O_8P_2Rh_2$	
Formula weight	916.48	
Temperature	150.00(10) K	
Wavelength	1.54184 Å	
Crystal system	Monoclinic	
Space group	$P2_1/n$	
Unit cell dimensions	a = 9.87390(5) Å	α = 90°
	b = 21.78333(8) Å	β = 102.6820(5)°
	c = 17.76504(7) Å	γ = 90°
Volume	3727.80(3) $Å^3$	
Z	4	
Density (calculated)	1.633 Mg/m^3	
Absorption coefficient	8.414 mm^{-1}	
F(000)	1856	
Crystal size	0.296 x 0.113 x 0.084 mm^3	
Theta range for data collection	4.059 to 72.910°	
Index ranges	-10<=h<=12, -26<=k<=27, -22<=l<=21	
Reflections collected	77133	
Independent reflections	7423 [R(int) = 0.0237]	
Completeness to theta = 67.684°	100.0 %	
Absorption correction	Gaussian	
Max. and min. transmission	1.000 and 0.554	
Refinement method	Full-matrix least-squares on F^2	
Data / restraints / parameters	7423 / 0 / 475	
Goodness-of-fit on F^2	1.127	
Final R indices [I>2sigma(I)]	R1 = 0.0201, wR2 = 0.0492	
R indices (all data)	R1 = 0.0202, wR2 = 0.0493	
Extinction coefficient	n/a	
Largest diff. peak and hole	0.435 and -0.365 e.$Å^{-3}$	